

# SCALE MICROFOSSILS FROM THE MID-NEOPROTEROZOIC FIFTEENMILE GROUP, YUKON TERRITORY

PHOEBE A. COHEN<sup>1,2</sup> AND ANDREW H. KNOLL<sup>3</sup>

<sup>1</sup>Department of Earth, Atmospheric and Planetary Sciences, Massachusetts Institute of Technology, Cambridge, MA 02139, USA;

<sup>2</sup>Department of Geosciences, Williams College, Williamstown, MA 01267, USA <Phoebe.A.Cohen@Williams.edu>; and

<sup>3</sup>Department of Organismic and Evolutionary Biology, Harvard University, Cambridge, MA 02138, USA <aknoll@oeb.harvard.edu>

**ABSTRACT**—Microscopic phosphatic scales are found in limestones and cherts from the 812–717 million year old Fifteenmile Group of the Yukon Territory. These enigmatic microfossils, which to date have not been identified in any other locality, display a diversity of intricate morphologies. Here we describe six new genera containing 17 new species of scale microfossils obtained from macerated limestone. We also revise existing taxa described originally from chert thin sections and now additionally freed from limestone by acid dissolution. New taxa described here are: *Archaeoxybaphon serratacapacis* n. sp., *Archeoxybaphon serratapusilla* n. sp., *Paleoscutula inornata* n. gen. n. sp., *Paleoscutula serrata* n. gen. n. sp., *Paleoscutula convocationis* n. gen. n. sp., *Hexacatillus allmonii* n. gen. n. sp., *Hexacatillus retetantillus* n. sp., *Quadrireticulum allisoniae* n. gen. n. sp., *Quadrireticulum palmaspinosum* n. gen. n. sp., *Circidentatus pistricis* n. gen. n. sp., *Circidentatus variodentatus* n. gen. n. sp., *Ospercapatera awramikii* n. gen. n. sp., *Circitorquis soccus* n. gen. n. sp., *Paleohexadictyon alexandrae* n. sp., *Paleomegasquama arctoa* n. sp., *Petasisquama petasus* n. sp., and *Thorakidictyon circireticulum* n. gen. n. sp. Taxa described or amended here are *Characodictyon skolopium* Allison and Hilgert, 1986, *Paleohexadictyon myriotrematum* Allison and Hilgert, 1986, *Archeoxybaphon polykeramoides* (Allison and Hilgert, 1986) emend., *Paleohexadictyon litosum* (Allison and Hilgert, 1986) emend., and *Thorakidictyon myriocanthum* (Allison and Hilgert, 1986) n. comb. Many eukaryotic clades include species with surficial scales but none provides a close morphological analog to the Fifteenmile scales. Nonetheless, comparative and functional morphology suggest that the diversification of heavily armored and morphologically complex cell-coverings records a changing ecological landscape in Neoproterozoic seas.

## INTRODUCTION

OVER THE last two decades our understanding of the Neoproterozoic fossil record has changed dramatically. Where once little evidence of evolution and diversity could be seen, we now observe innovation and turnover, documenting biological events that collectively set the stage for the Ediacaran and Cambrian transformation of marine ecosystems (Knoll et al., 2006; Macdonald et al., 2010a). New fossil records, integrated with improving eukaryotic phylogenies, molecular clocks, geochemical records, and geochronometric constraints provide unprecedented clarity (and new questions) about early eukaryotic evolution. Collectively, the microfossil record indicates that between the onset of the Bitter Springs isotopic stage (~811.5 Ma) and the Sturtian glaciation (~716.5 Ma), many major eukaryotic crown groups diversified, including rhizarians, amoebozoans, and both red and green algae.

Among the most enigmatic and intriguing records of pre-Sturtian eukaryotic diversity are scale microfossils from the Fifteenmile Group, Yukon Territory, first described by Allison and Hilgert (1986). Originally identified in thin sections of early diagenetic chert nodules, the scales were presumed to be siliceous analogous to broadly comparable structures made by living chrysophytes. Cohen et al. (2011), however, showed that the scales are actually phosphatic and can be recovered by acid dissolution of carbonates in the Fifteenmile succession. This, in turn, enables individual fossils to be imaged via SEM, providing new insights into scale morphology.

Here we describe new taxa found in the beds originally studied by Allison and Hilgert (1986) and Cohen et al. (2011) as well as fossils from five additional horizons lower in the same section. These new taxa greatly increase the observed morphological diversity of mineralized microfossils from Fifteenmile beds. Additionally, we revise the taxonomy of previously described taxa based on the increased morphological resolution

available in specimens freed from carbonates. The Fifteenmile scale microfossil assemblage represents the most morphologically complex and diverse group of pre-Ediacaran protists described to date, adding substantially to the growing record of early- to mid-Neoproterozoic eukaryotic diversity.

## GEOLOGICAL SETTING AND AGE

**Stratigraphy.**—The Fifteenmile Group lies within the Macenzie Mountain Supergroup and is exposed across the southern Ogilvie Mountains of Eastern Yukon and Western Alaska (Macdonald et al., 2011). The fossiliferous section is exposed in the Tatonduk Inlier, a wedge of relatively unmetamorphosed sedimentary rocks deposited along the margin of Laurentia and exposed today in outcrops that straddle the Alaska-Yukon border (Fig. 1.1). The scale microfossils are tentatively assigned to the Craggy Dolomite Formation of the Fifteenmile Group, exposed at Mt. Slipper (Figs. 1.1, 2). Here, some 670 m of mixed carbonate and shale are exposed on the east flank of an anticline above a valley that drains to Tindir Creek. Fossils are found in the upper unit of the Mt. Slipper section, a ~173 m succession of dark gray limestone rhythmite with interbedded shale. The Tindir scales were first identified in early diagenetic chert nodules from a ~3 m section near the top of this unit; subsequently, additional assemblages described here were discovered in organic-rich limestones from ~60 m of section within the upper unit and below the original horizon (Cohen et al., 2011; Fig. 1.3). The fossiliferous facies is interpreted as a shallow subtidal deposit within a shallowing-upward sequence. See Macdonald et al. (2010b, 2011) and Cohen et al. (2011) for additional discussion of stratigraphic setting.

**Age constraints.**—Microfossils were first described from the Fifteenmile Group (as the Tindir Formation; see Macdonald et al., 2010a, 2011, for changes in stratigraphic nomenclature) by Allison and co-authors (Allison and Moorman, 1973; Allison and Hilgert, 1986; Allison and Awramik, 1989). Allison and colleagues described a diverse assemblage of microfossils from

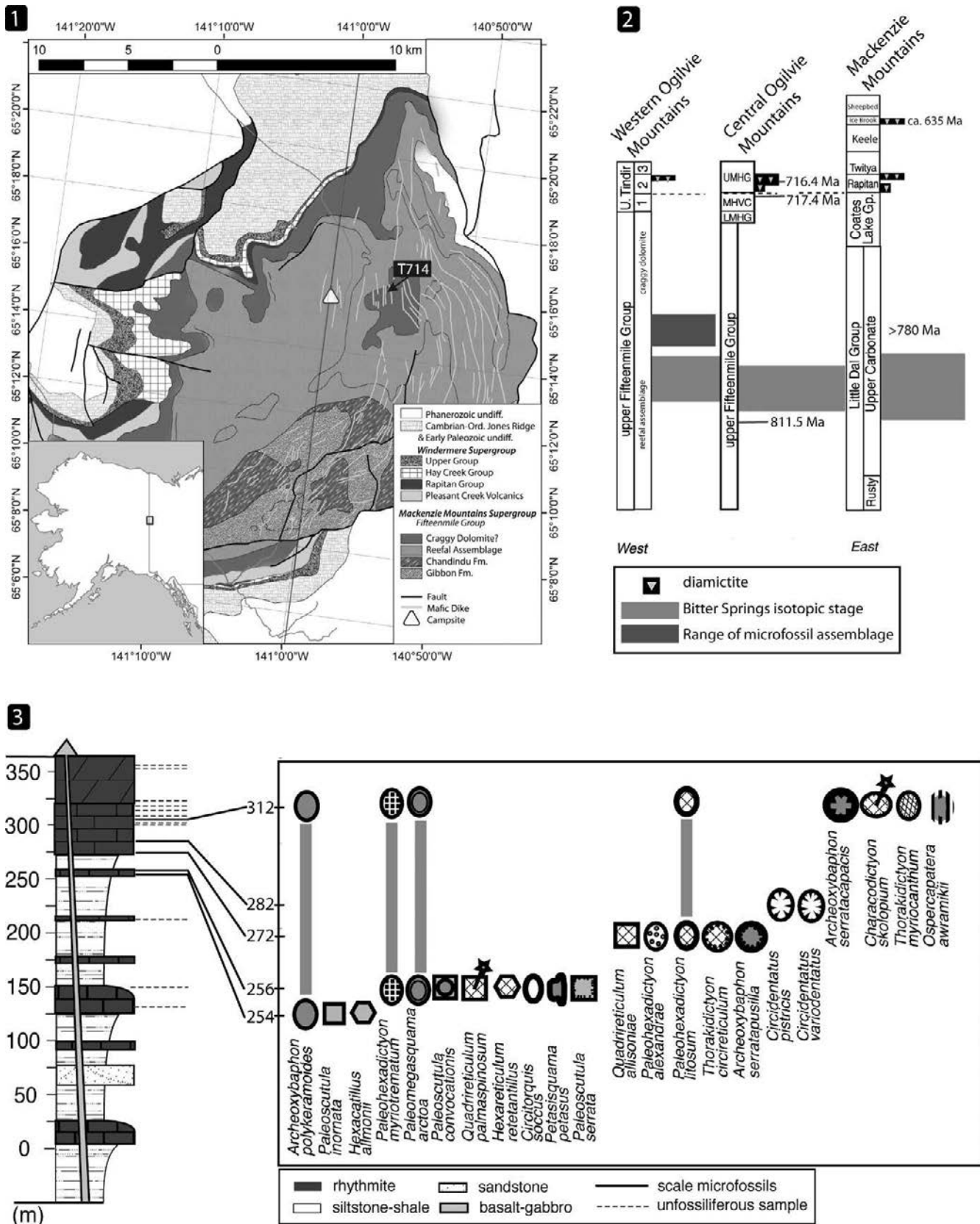


FIGURE 1—Geologic setting for the Fifteenmile taxa. 1, geologic map of the Fifteenmile Group and associate strata of the Western Ogilvie Mountains (adapted from Cohen et al., 2011); inset shows approximate geographic location of the map along the Alaska-Yukon boarder; 2, overview of the regional stratigraphy and age constraints on the fossiliferous unit; 3, fossiliferous section T714 showing the stratigraphic distribution of carbonate-hosted scale taxa as well as the location of unfossiliferous sample horizons. Abbreviations: UMHG=Upper Mount Harper Group; MHVC=Mount Harper Volcanic Complex; LMHG=Lower Mount Harper Group. See Macdonald et al. (2010a, 2010b) for references and additional information.

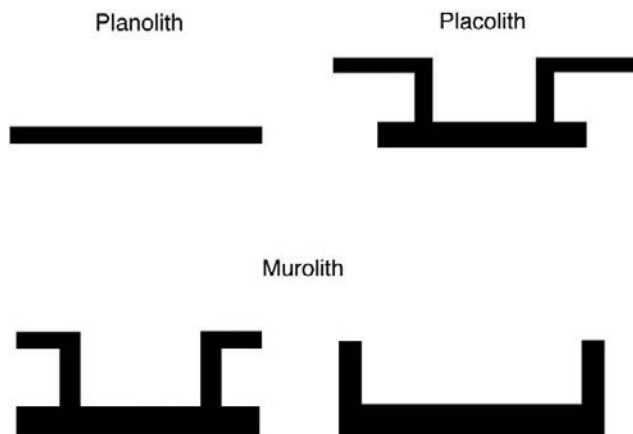


FIGURE 2—Explanations of morphology terms used in species descriptions, adapted from those used for coccolithophores in Cross and Fortuno (2002).

limestone-hosted chert nodules, including putative coccoidal cyanobacteria, cyanobacterial filaments, leiosphaerid, and acanthomorphic acritarchs, vase-shaped microfossils, and scale microfossils, hypothesized to be siliceous. Allison argued that the fossiliferous unit was early Cambrian in age, while Hilgert interpreted it as Ediacaran, both basing their arguments on proposed bio- and lithostratigraphic correlations.

Kaufman et al. (1992) provided chemostratigraphic support for a Neoproterozoic age, based on Sr isotopic abundances distinct from those known for Cambrian or Ediacaran carbonates. Subsequent work by Macdonald et al. (Macdonald et al., 2010a, 2011) demonstrated that the fossiliferous unit lies not in the upper Tindir Formation, as initially described, but in the lower Tindir rocks, now re-assigned to the lower assemblage of the Fifteenmile Group. Macdonald et al. (2010a, 2010b) also provided improved chemostratigraphic and radiometric control that brackets the fossiliferous unit between  $811.5 \pm 0.25$  and  $717.43 \pm 0.14$  Ma (Fig. 1.2). These dates are consistent with acanthomorphic acritarchs and vase-shaped microfossils reported from Fifteenmile cherts by Allison and Awramik (1989), which are typical for early to mid-Neoproterozoic strata.

#### MATERIAL AND METHODS

Samples were collected from measured stratigraphic sections in June 2007, at N  $65^{\circ}16'$ , W  $140^{\circ}57'$  (Fig. 1.1). Fossils were obtained from six limestone samples distributed through 60 m of the upper Fifteenmile Formation (Fig. 1.3). Dozens of additional samples proved unfossiliferous (Fig. 1.3).

Hand samples were broken into  $\sim 2$  cm<sup>3</sup> pieces and dissolved in 30% acetic acid; the resulting macerates were filtered through a 30- $\mu$ m mesh, dry-mounted on copper or carbon tape with or without an SEM finder grid, and coated with Pt/Pd or Au for study by SEM, FIB-SEM, and EDS. SEM images were acquired using a Zeiss Supra FE-SEM, Zeiss Ultra FE-SEM, or a Nanovision FIB-SEM.

#### SYSTEMATIC PALEONTOLOGY

Allison and Hilgert (1986) provide a detailed taxonomic treatment of Fifteenmile scale microfossils preserved in chert, and thus the taxonomy presented here follows their lead in separating genera on the basis of overall shape, plate characteristics, and the presence, absence, and, if present, nature of spines for taxon identification. Terminology developed for the description of coccolith plates facilitates discussion of the Fifteenmile scales and so are employed here (Fig. 2). All

specimens described here are from acid maceration residues and have been examined with SEM. All type and illustrated specimens have been deposited with the Yukon Paleontology Program, Whitehorse, Yukon under accession numbers YG#418.1–YG#418.46.

#### EUKARYA INCERTAE CEDIS

#### Genus ARCHEOXYBAPHON Allison and Hilgert, 1986

*Type species.*—*Archeoxybaphon polykeramoides* ALLISON AND HILGERT, 1986.

*Diagnosis.*—Original: Scales imperforate, all of one morphology and approximate size. Outline elliptic, very slightly domed when observed in side view. Cluster exhibits overlapping of scales in more than one direction. Emended: Scales imperforate, outline elliptic to circular, very slightly domed when observed in side view. Cluster exhibits overlapping of scales in more than one direction.

#### ARCHEOXYBAPHON POLYKERAMOIDES emend.

#### Figure 3.1–3.6

1986 *Archeoxybaphon diminutum* ALLISON AND HILGERT, p. 987, fig. 5.5.

1986 *Archeoxybaphon amydrum* ALLISON AND HILGERT, p. 987, fig. 5.3, 5.4.

*Diagnosis.*—Original: Scales imperforate, all of one morphology and approximate size. Outline elliptic, very slightly domed when observed in side view. Cluster exhibits overlapping of scales in more than one direction. Emended: Planolith, elliptical scales, ca. 20–25  $\mu$ m in maximum dimension, imperforate, slightly domed, with a thin rim around the concave surface. Scales overlapping when found in clusters.

*Description.*—Mean length, 20.6  $\mu$ m (maximum 27.6  $\mu$ m, minimum 14.3  $\mu$ m, standard deviation 5.8  $\mu$ m); mean width 17.3  $\mu$ m (maximum 23.9  $\mu$ m, minimum 12.2  $\mu$ m, standard deviation 5.5  $\mu$ m); mean rim width 0.8  $\mu$ m; N=18.

*Material examined.*—Eighteen complete specimens from meters 252, 256, 312.

*Remarks.*—Allison and Hilgert (1986) erected three species of *Archeoxybaphon*, differing mainly in size. Measurements of macerated samples suggest a continuous size distribution (Fig. 4); thus, we have synonymized the three taxa, retaining the name of the type species. Scales found individually, in stacks, and in clusters.

#### ARCHEOXYBAPHON SERRATACAPACIS new species

#### Figure 5.1–5.4

*Diagnosis.*—A species of *Archeoxybaphon* with roughly equilateral triangular teeth projecting inward from the rim on the concave face.

*Description.*—Planolith, broadly elliptical scale, imperforate, with flat central area. Teeth project inward from the rim around the concave face and lie flat against the plate surface. High magnification shows small gaps where teeth are attached to the rim of the plate; it appears that the teeth are composite structures built by the merger of originally thin projections. Teeth are triangular in shape and roughly equilateral. Mean plate diameter 31.3  $\mu$ m (maximum 33.7  $\mu$ m, minimum 28.1  $\mu$ m); mean length of edge teeth, 2.9  $\mu$ m (maximum 4.3  $\mu$ m, minimum 2.1  $\mu$ m); N=6.

*Etymology.*—From the Latin *serrata*, meaning toothed, and *capacis*, meaning wide.

*Types.*—Holotype YG#418.6 (Fig. 5.1, 5.2) from sample T714-312 (SEM stub 312-g-1), Neoproterozoic Mount Slipper locality, Fifteenmile Group, Yukon Territory.

*Material examined.*—Six specimens, meter 312.

*Occurrence.*—Fifteenmile Group, Mount Slipper, Section T714, meter 312, Yukon Territory.

*Remarks.*—Plates often found in overlapping stacks.

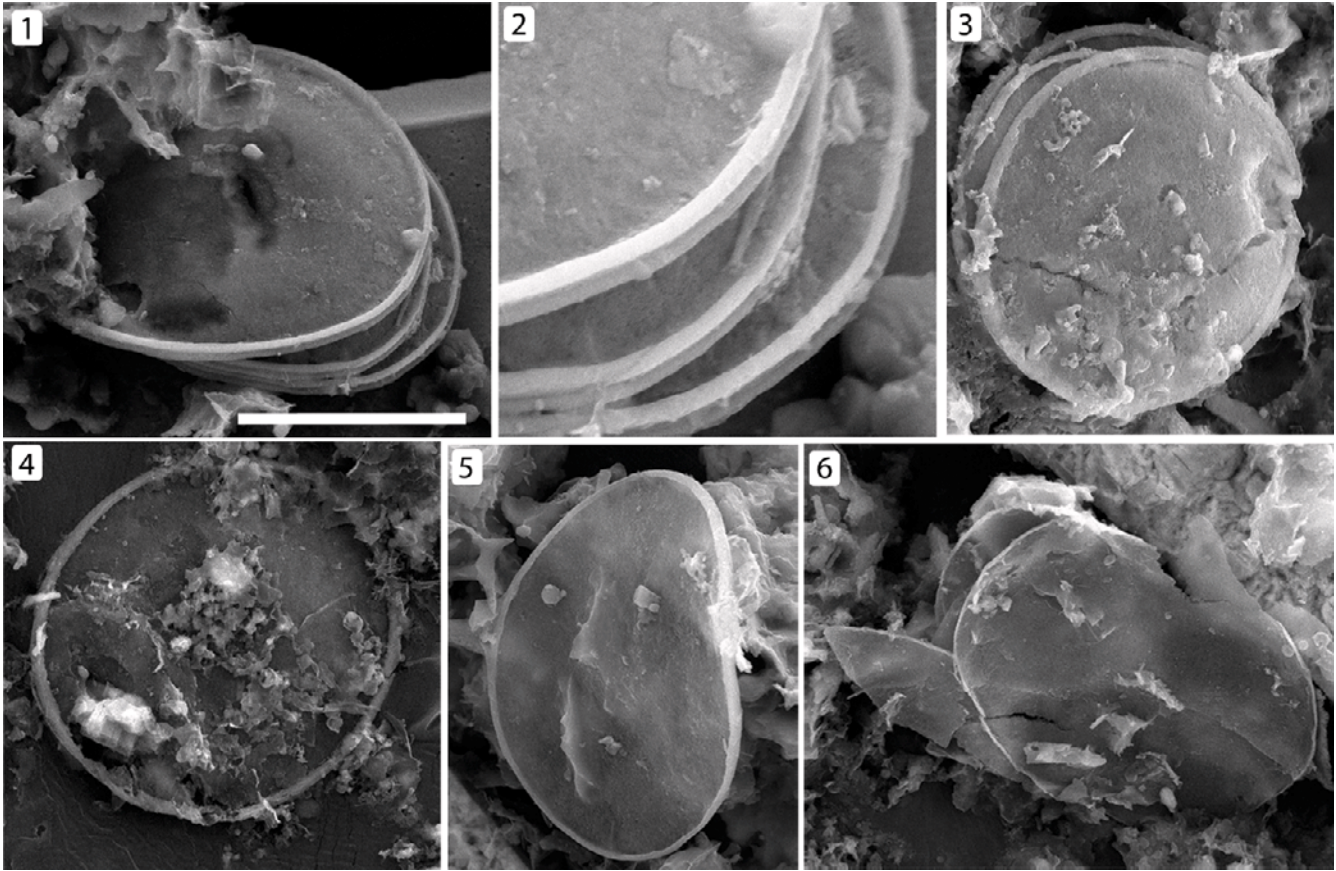


FIGURE 3—*Archeoxybaphon polykeramoides* (Allison and Hilgert, 1986) emend. 1, YG#418.1 (SEM stub 312-g2); 2, detail of 1 showing the edges of three stacked plates; 3, YG#418.2 (SEM stub 256-g9-); 4, YG#418.3 (SEM stub 256-g6); 5, YG#418.4 (SEM stub 256-g6); 6, YG#418.5 (SEM stub 252-g2). Scale bar is 20  $\mu\text{m}$  in 1; 5  $\mu\text{m}$  in 2; 15  $\mu\text{m}$  in 3; 12  $\mu\text{m}$  in 4; 9  $\mu\text{m}$  in 5; 14  $\mu\text{m}$  in 6.

ARCHEOXYBAPHON SERRATAPUSILLUM new species

Figure 5.5, 5.6

**Diagnosis.**—A species of *Archeoxybaphon* with small teeth along the scale rim.

**Description.**—Broadly elliptical, planolith, flat, solid plate with acicular teeth projecting inward from the outer edge of the rim. Rim only slightly raised over the plane of the central area. Rim appears curled over the edge of the plate and extends approximately half way towards the center of the plate. Plate diameter 24.5  $\mu\text{m}$ ; rim width, 0.4  $\mu\text{m}$ ; edge spine length, 0.5  $\mu\text{m}$ ; N=1.

**Etymology.**—From the Latin *serrata*, meaning toothed, and *pusillum*, meaning tiny.

**Types.**—Holotype YG#418.8 (Fig. 5.5, 5.6) from sample T714-272 (SEM stub 272-g-1), Neoproterozoic Mount Slipper locality, Fifteenmile Group, Yukon Territory.

**Material examined.**—One specimen, meter 272.

**Occurrence.**—Fifteenmile Group, Mount Slipper, Section T714, Yukon Territory.

**Remarks.**—*Archeoxybaphon serratapusillum* differs from other species of *Archeoxybaphon* by its sharp narrow teeth and broad rim. Specimens found stacked on top of each other.

Genus CHARACODICTYON Allison and Hilgert, 1986

**Type species.**—*Characodictyon skolopium* Allison and Hilgert, 1986.

CHARACODICTYON SKOLOPIUM Allison and Hilgert, 1986.

Figure 6

1986 *Characodictyon skolopium* ALLISON AND HILGERT, p. 986, fig. 6.7, 6.8.

1986 *Characodictyon diskolopium* ALLISON AND HILGERT, p. 993, fig. 7.1–7.3.

1986 *Characodictyon diskolopium* var. *circula* ALLISON AND HILGERT, p. 993, fig. 7.4, 7.5.

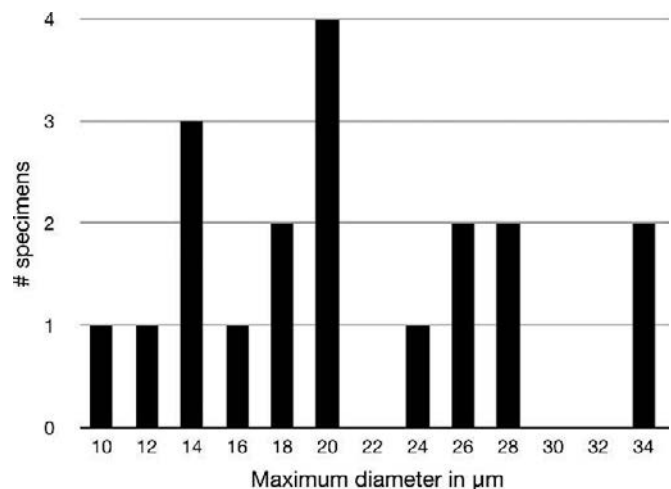


FIGURE 4—Histogram of the size distribution of *Archeoxybaphon polykeramoides* (Allison and Hilgert, 1986) emend. Bins are 2  $\mu\text{m}$  in size and measurements were rounded to 0.1  $\mu\text{m}$ ; N=23.

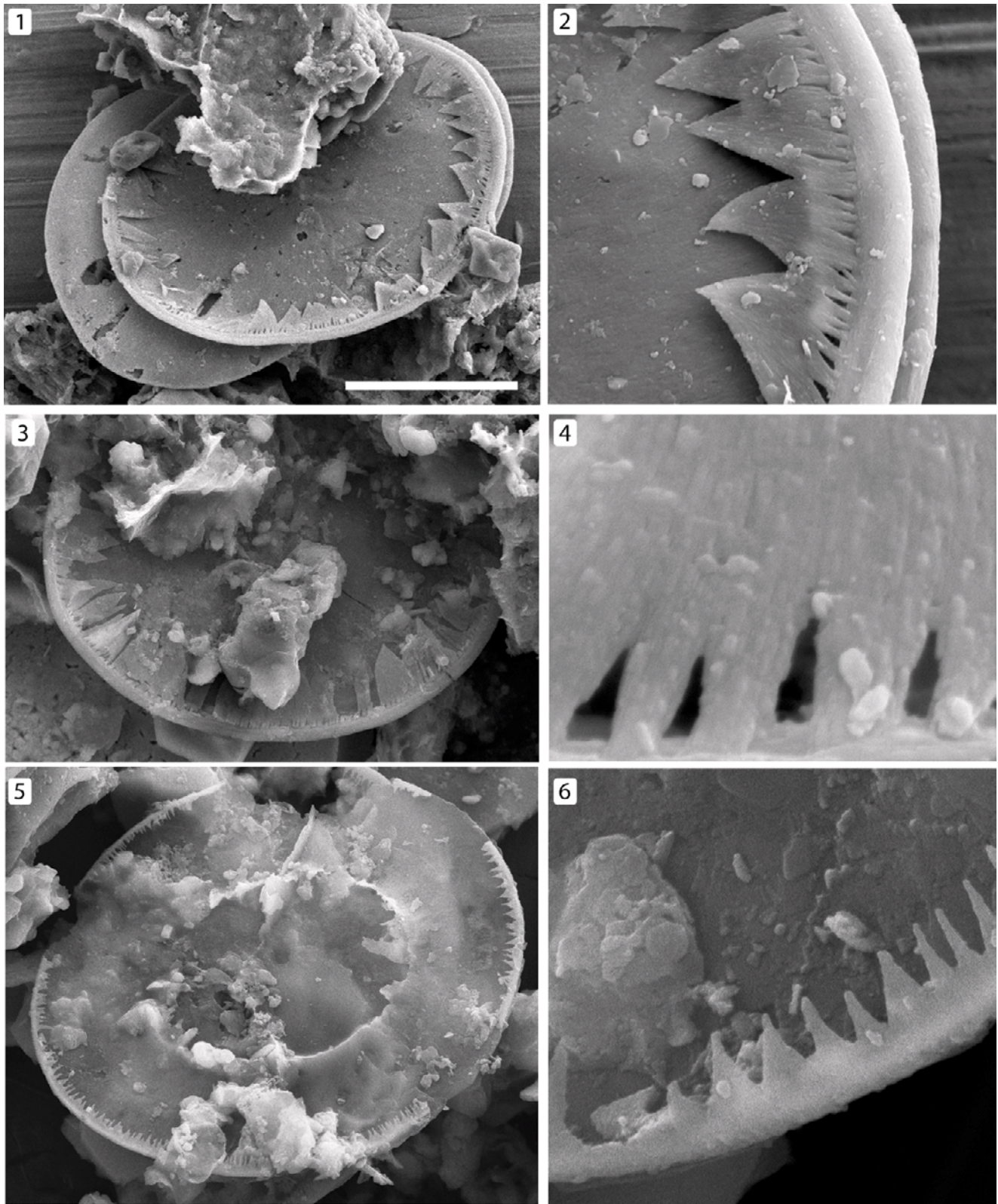


FIGURE 5—1–4, *Archeoxybaphon serratacapacis* n. sp. 1, YG#418.6 (SEM stub 312-g-1); two scales, stacked; note teeth are present on only one surface; 2, detail of edge teeth from 1; 3, YG#418.7 (SEM stub 312-g-2), specimen shows slightly degraded edge teeth; 4, detail of teeth from 3 showing spacing at connecting interface between the teeth and the plate rim; 5, 6, *Archeoxybaphon serratapusillum* n. sp.: 5, YG#418.8 (SEM stub 272-g-1); 6, detail of 5 showing teeth rimming the edge of the scale. Scale bar is 15  $\mu\text{m}$  in 1; 3  $\mu\text{m}$  in 2; 12  $\mu\text{m}$  in 3; 500 nm in 4; 15  $\mu\text{m}$  in 5; 3  $\mu\text{m}$  in 6.

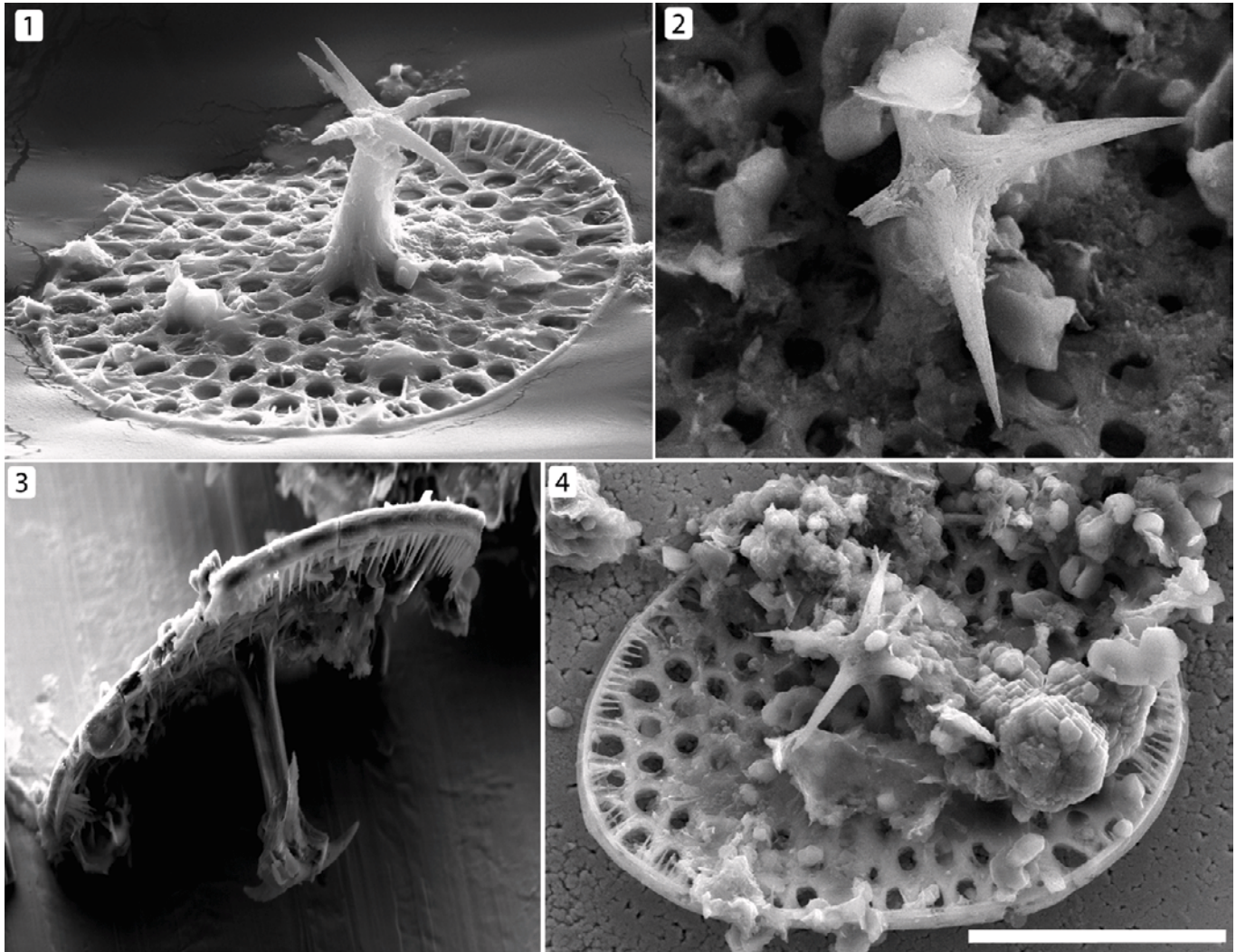


FIGURE 6—*Characodictyon skolopium* (Allison and Hilgert, 1986). 1, YG#418.9 (SEM stub 312-stub3) specimen showing central boss with three distinct spines and one bifurcated spine; 2, YG#418.10 (SEM stub 312-stub10); 3, YG#418.11 (SEM stub 312-stub12); 4, YG#418.12 (SEM stub 312-stub12). Scale bar is 15  $\mu\text{m}$  for 1, 3, 4; 8  $\mu\text{m}$  in 2.

1986 *Characodictyon skolopium* var. *soleniscum* ALLISON AND HILGERT, p. 993, fig. 6.11.

1986 *Characodictyon skolopium* var. *tetragonum* ALLISON AND HILGERT, p. 993, fig. 6.9, 6.10.

**Description.**—Elliptical plate with prominent pores arranged in hexagonal close-packing. Rim slightly elevated above the surface of one side of the plate. Acicular spines present around the edge of the scale, facing inwards at almost a right angle so that spines run nearly parallel to the surface of the plate. Spines also present on struts that define pore intersections, each intersection spine extending upwards at a right angle from the surface of the plate. A single boss-like structure extends at a right angle from the center of one side of the flat plate, terminating in an anchor-like structure. Anchor has 4 to 6 spines radiating out in a slightly uneven pattern from the distal end. Spines curve gently downwards from base to tip. Mean plate length, 42.5  $\mu\text{m}$  (maximum 52.4  $\mu\text{m}$ , minimum 26.2  $\mu\text{m}$ , standard deviation 8.8  $\mu\text{m}$ ); mean plate width, 25.8  $\mu\text{m}$  (maximum 33.8  $\mu\text{m}$ , minimum 21.4  $\mu\text{m}$ , standard deviation 4.7  $\mu\text{m}$ ); mean plate length-to-width ratio, 0.63; mean pore diameter, 1.7  $\mu\text{m}$ ; pore intersection spine length, 0.8–1.5  $\mu\text{m}$ ; mean edge spine length, 2.4  $\mu\text{m}$ ; mean central spine length, 7.5  $\mu\text{m}$ ; central spine width, 1.5–2.5  $\mu\text{m}$ ; mean

anchor point length, 5.4  $\mu\text{m}$ , maximum, 6.6  $\mu\text{m}$ , minimum, 3.8  $\mu\text{m}$ ; N=5.

**Material examined.**—Five complete specimens, three partial.

**Occurrence.**—Fifteenmile Group, Mount Slipper, Section T714, meter 312, Yukon Territory.

**Remarks.**—This population was previously observed only in thin section. Edge spines and pore intersection spines, prominent in SEM micrographs, cannot be resolved in thin sections images. Allison and Hilgert (1986) differentiated two species and an additional subspecies based on apparent variations in central spine morphology. SEM examination of macerated specimens indicates that apparent differences reflect diagenesis and petrographic artifact. Chert-hosted specimens show variation in coloration and the distribution of carbonaceous material to mineralized material, which can make areas of the scales appear hollow, whereas in the limestone hosted specimens, all central spine shafts observed are solid. Thus, *Characodictyon skolopium* var. *soleniscum* is here subsumed into *C. skolopium*. Similarly, we believe that *C. diskolopium* also belongs within *C. skolopium* because variation in spine number and angle along with the vagaries of diagenesis could potentially give the impression of spines at different levels along the central shaft when in fact, in limestone hosted specimens, we see no evidence of such

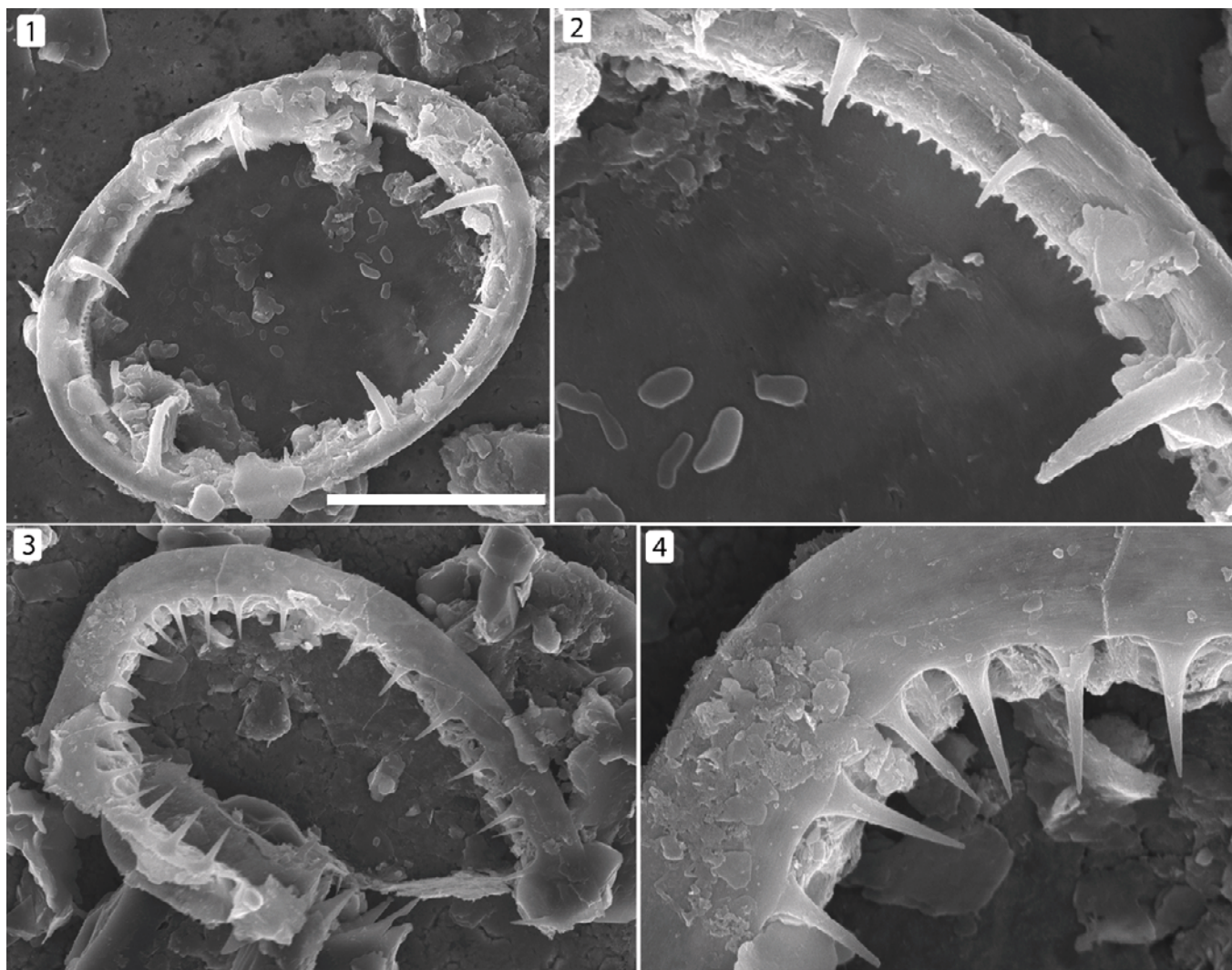


FIGURE 7—1, 2, *Circidentatus variodentatus* n. gen. n. sp. 1, YG#418.14 (SEM stub 282-g2); 2, detail of 1 showing edge spines of two different lengths; 3, 4, *Circidentatus pistricis* n. gen. n. sp.; 3, YG#418.13 (SEM stub 282-g2); 4, detail of 3 showing edge spines. Scale bar is 7  $\mu$ m in 1; 4  $\mu$ m in 2; 7  $\mu$ m in 3; 2  $\mu$ m in 4.

variation. Additionally, low rims are observed in all limestone-hosted specimens of *C. skolopium*, negating this proposed difference between species as well. *Characodictyon diskolopium* var. *circula* and *C. skolopium* var. *tetragonum* are additionally subsumed into *C. skolopium* because we see no distinct populations of specimens with regard to outline shape; instead we believe more rounded or rectangular forms fall within the natural variation of the taxa. See Table 1 and Table 2 for additional information on genus assignments. Scales often found individually but occasionally are found in stacks or clusters.

#### Genus CIRCIDENTATUS new genus

*Type species.*—*Circidentatus pistricis* n. sp.

*Other species.*—*Circidentatus variodentatus* n. sp.

*Diagnosis.*—Oval ring-shaped scale with no central plate. Spines in one or two rows extending from ring toward scale center. Murolith form, lacking flanges, with a wide wall.

*Etymology.*—From the Latin *circus* for ring or oval used for races and *dentatus* for toothed.

*Remarks.*—It is difficult to determine if the hollow center of this form is an original feature or results from diagenetic loss of a thin plate; however, no vestige of a central plate has been observed.

#### CIRCIDENTATUS PISTRICIS new species

Figure 7.3, 7.4

*Diagnosis.*—A species of *Circidentatus* with spines of uniform length edging the rim.

*Description.*—Spines of equal length protrude from the rim of the scale toward the center. Spines curve downwards from rim edge. Maximum diameter, 17.8  $\mu$ m; spine length, 2.2  $\mu$ m; space between spines 1–2  $\mu$ m; N=1.

*Etymology.*—From the Latin *pistris*, meaning shark or sea-monster, for the formidable set of tooth-like spines that project from the outer rim.

*Types.*—Holotype YG#418.13 (Fig. 7.3, 7.4) from sample T714-282 (SEM stub 282-g-2), Neoproterozoic Mount Slipper locality, Fifteenmile Group, Yukon Territory.

*Material examined.*—One partial specimen, meter 282.

*Occurrence.*—Fifteenmile Group, Mount Slipper, Section T714, Yukon Territory.

*Remarks.*—Only one isolated specimen of this taxon has been found.

#### CIRCIDENTATUS VARIODENTATUS new species

Figure 7.1, 7.2

TABLE 1—List of all genera of scale microfossils from section T714, Fifteenmile Group. Taxa are categorized by the lithology in which they are found as well as by over-arching morphological features. All chert-hosted fossils are from Allison and Hilgert, 1986; carbonate-hosted taxa are described here.

Taxon	Lithology	Shape	Surface	Spines
<i>Archeoxybaphon serratacapacis</i>	Carbonate	Hexagonal	Solid	Edge
<i>Archeoxybaphon serratapusillum</i>	Carbonate	Round	Solid	Edge
<i>Circidentatus pistricis</i>	Carbonate	Oval	Hollow	Edge
<i>Circidentatus variodentatus</i>	Carbonate	Oval	Hollow	Edge
<i>Circitorquis soccus</i>	Carbonate	Oval	Hollow	None
<i>Hexacatillus allmonii</i>	Carbonate	Hexagonal	Solid	None
<i>Hexareticulum retetantillus</i>	Carbonate	Hexagonal	Perforate	None
<i>Ospercapatera awramikii</i>	Carbonate	Oval	Solid	None
<i>Paleohexadictyon alexandrae</i>	Carbonate	Oval	Perforate	None
<i>Paleomegasquama arctoa</i>	Carbonate	Oval	Solid	None
<i>Paleoscutula convocationis</i>	Carbonate	Square	Solid	None
<i>Paleoscutula inornata</i>	Carbonate	Square	Solid	None
<i>Paleoscutula serrata</i>	Carbonate	Square	Solid	Edge
<i>Petasisquama petasus</i>	Carbonate	Oval	Solid	None
<i>Quadrirreticulum allisoniae</i>	Carbonate	Square	Perforate	None
<i>Quadrirreticulum palmaspinosum</i>	Carbonate	Square	Perforate	Central
<i>Thorakidictyon circireticulum</i>	Carbonate	Round	Perforate	Edge
<i>Archeoxybaphon polykeramoides</i>	Chert/carbonate	Round	Solid	None
<i>Bicorniculum brockum</i>	Chert/carbonate	Oval	Hollow	Edge/none
<i>Characodictyon skolopium</i>	Chert/carbonate	Oval	Perforate	Edge/central
<i>Thorakidictyon myriocanthum</i>	Chert/carbonate	Oval	Perforate	Edge
<i>Paleohexadictyon litosum</i>	Chert/carbonate	Oval	Perforate	None
<i>Paleohexadictyon myriotrematum</i>	Chert/carbonate	Oval	Perforate	None
<i>Altarmilla multistriata</i>	Chert	Oval	Solid/perforate	None
<i>Aqualisquama centritubula</i>	Chert	Oval	Solid	None
<i>Confinisquama fimbriata</i>	Chert	Oval	Solid	None
<i>Hyaloxybaphon monokeramoides</i>	Chert	Oval	Solid	None
<i>Invaginatalteus depressus</i>	Chert	Oval	Solid	None
<i>Invaginatalteus dimorphus</i>	Chert	Oval	Solid/perforate	None
<i>Paleocrassilimbus spinosus</i>	Chert	Oval	Solid	Edge
<i>Paleomegasquama coccolithoides</i>	Chert	Oval	Solid	None
<i>Paterasquama crassa</i>	Chert	Oval	Perforate	None
<i>Patinisquama cirratomarginata</i>	Chert	Oval	Perforate	None
<i>Petasisquama alta</i>	Chert	Oval	Solid	None
<i>Petasisquama laciniata</i>	Chert	Oval	Solid	None
<i>Petasisquama versicorona</i>	Chert	Oval	Solid	None
<i>Radiocerniculum inornatum</i>	Chert	Oval	Perforate	None
<i>Spinicerniculum tribulosum</i>	Chert	Oval	Perforate	Central

**Diagnosis.**—A species of *Circidentatus* with two sizes of teeth edging different planes of the rim.

**Description.**—Two sets of spines extend in distinct planes from the outer rim toward the center, one set much longer than the other. Longer spines curve downwards from the rim edge. Maximum diameter 20.6  $\mu\text{m}$ ; minimum diameter, 16.7  $\mu\text{m}$ ; ratio of width to length, 0.75; long spine length, 2.2  $\mu\text{m}$ ; short spine length, 100 nm; N=1.

**Etymology.**—From the Latin *vario*, meaning different, and *dentatus*, meaning toothed, for the fact that this species has two distinct sets of differently sized teeth-like structures.

**Types.**—Holotype YG#418.14 (Fig. 7.1, 7.2) from sample T714-282 (SEM stub 282-g-2), Neoproterozoic Mount Slipper locality, Fifteenmile Group, Yukon Territory.

**Material examined.**—One specimen from meter 282.

**Occurrence.**—Fifteenmile Group, Mount Slipper, Section T714, Yukon Territory.

**Remarks.**—Only one specimen of this taxon has been found. The larger spines in *C. variodentatus* vary more in length than those of *C. pistris*.

#### CIRCITORQUIS new genus

**Type species.**—*Circitorquis soccus* n. sp. by monotypy.

**Diagnosis.**—Oval ring-shaped scale. Murolith form with upper and lower flanged surfaces separated by a vertical wall.

**Etymology.**—Latin *circus* for oval and *torquis* for ring.

**Remarks.**—*Circitorquis* can be differentiated from other ovoid forms with no central plate by its conspicuous paired flanges.

#### CIRCITORQUIS SOCCUS new species

Figure 8.1–8.3

**Diagnosis.**—A species of *Circitorquis*, 34 to 50  $\mu\text{m}$  in maximum dimension.

**Description.**—Oval scale consisting of a wide rim with a flatted top and bottom surface and an inwardly curved, concave edge. No central plate. Upper and lower flanges protrude slightly. Some flanges appear to be edged by a thin band with sub-micron teeth (Fig. 13.2). Mean maximum scale length 41.4  $\mu\text{m}$  (maximum 47.4  $\mu\text{m}$ , minimum, 34.1  $\mu\text{m}$ ); mean scale width 33.4  $\mu\text{m}$  (maximum 35  $\mu\text{m}$ , minimum 31.7  $\mu\text{m}$ ); mean lip thickness 6.1  $\mu\text{m}$  (maximum 6.7  $\mu\text{m}$ , minimum 5.6  $\mu\text{m}$ ); N=4.

**Etymology.**—From the Latin *soccus* meaning slipper, in reference to Mount Slipper, the locality where the Fifteenmile scale fossils were found.

**Types.**—Holotype YG#418.15 (Fig. 8.1) from sample T714-256 (SEM stub 256-g6), Neoproterozoic Mount Slipper locality, Fifteenmile Group, Yukon Territory.

TABLE 2—Clarification of the morphological and taxonomic distinction between genera of oval-to-round, porate, scales.

Genus	Hexagonal pores	Pore intersection spines	Edge spines	Central spine
<i>Characodictyon</i> Allison and Hilgert, 1986	Y	Y	Y	Y
<i>Chilodictyon</i> Allison and Hilgert, 1986	Y	Y/N	Y/N	N
<i>Paleohexadictyon</i> Allison and Hilgert, 1986	Y	N	N	N
<i>Thorakidictyon</i> gen. nov.	Y	Y	Y	N



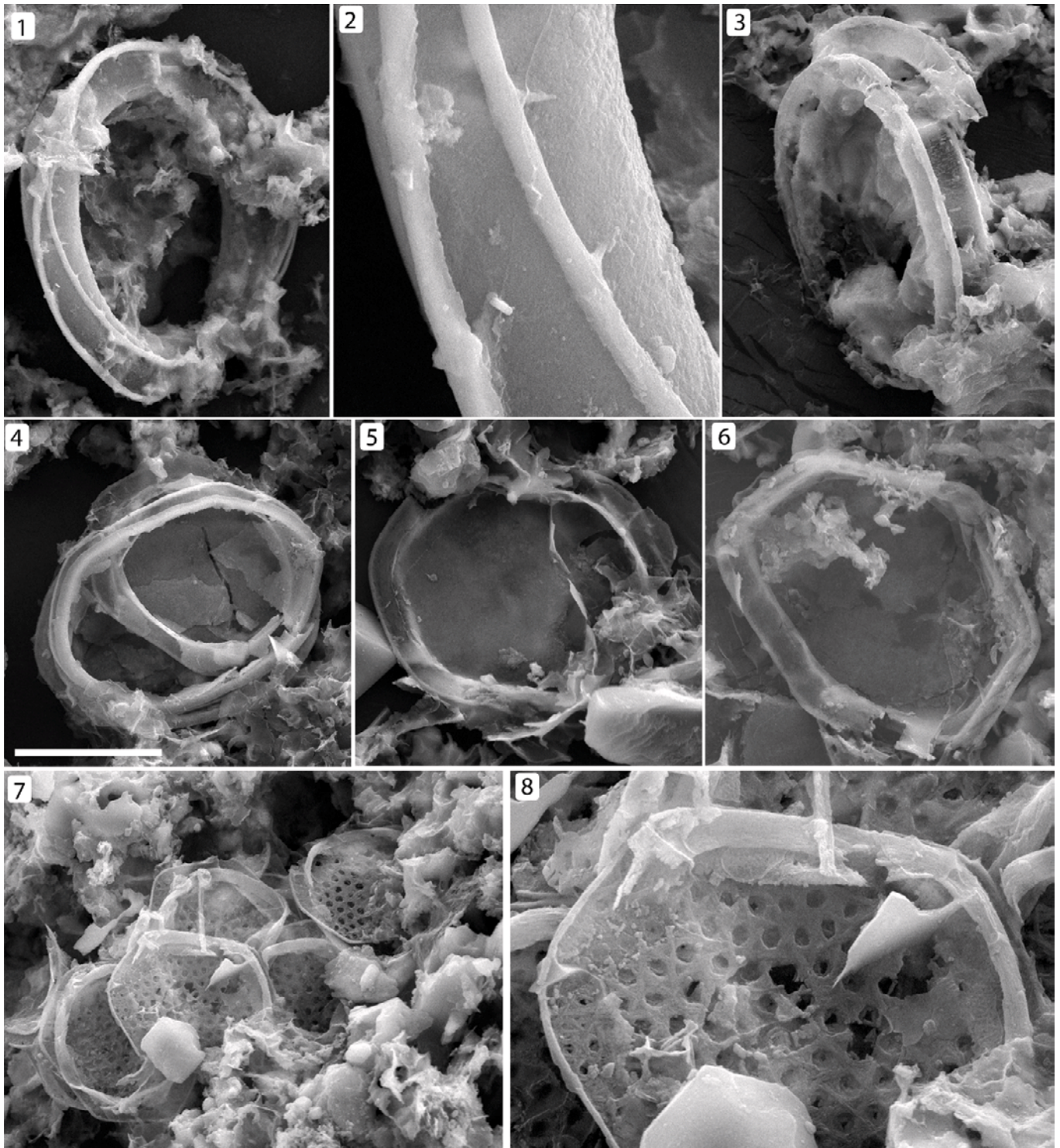


FIGURE 8—1–3, *Circitorquis soccus* n. gen n. sp.: 1, YG#418.15 (256-g6); 2, detail of edge of 1 showing narrow bands, possibly with teeth; 3, YG#418.16 (SEM stub 256-g6); 4–6, *Hexacatillus allmonii* n. gen n. sp.: 4, YG#418.17 (SEM stub 256-g8); 5, YG#418.18 (SEM stub 256-g8); 6, YG#418.19 (SEM stub 256-g8); 7, 8, *Hexareticulum retetantillus* n. gen n. sp.: 7, YG#418.20 (SEM stub 256-g8), cluster of specimens; 8, close-up of a single scale within cluster shown in 7. Scale bar is 12  $\mu$ m in 1; 4  $\mu$ m in 2; 12  $\mu$ m in 3; 7  $\mu$ m in 4; 10  $\mu$ m in 5; 10  $\mu$ m in 6; 12  $\mu$ m in 7; 4  $\mu$ m in 8.

*Material examined.*—Four complete specimens from meter 256.

*Occurrence.*—Fifteenmile Group, Mount Slipper, Section T714, Yukon Territory.

*Remarks.*—It is difficult to know whether a bottom surface of the scale was originally present and lost, or if the scale was

originally hollow in the center. It is also difficult to determine if the thin band seen in Figure 8.2 continues around the entire scale or is isolated to certain areas. Specimens found in isolation.

Genus HEXACATILLUS new genus

*Type species.*—*Hexacatillus allmonii* n. sp.

*Other species.*—*Hexacatillus retetantillus* n. sp.

*Diagnosis.*—A flat six-sided form with two hexagonal plates, one slightly smaller than the other, stacked on top of one another. Muroolith form with raised rim above the central area and distal and proximal flanges. Wall connecting the two surfaces curved concavely and often striated. Surfaces of hexagonal plates both either solid or reticulate.

*Etymology.*—From the Latin *hexa*, meaning a six-sided, and *catillus*, meaning small dish.

*Occurrence.*—Fifteenmile Group, Mount Slipper, Section T714, Yukon Territory.

*Remarks.*—Members of this genus are found in isolation, in groupings of two to three scales, and in larger clusters. Significant variation occurs in the length of plate edges within single specimens and between specimens. The angle between each plate edge also varies between specimens.

#### HEXACATILLUS ALLMONII new species

Figure 8.4–8.6

*Diagnosis.*—A species of *Hexacatillus* with solid surfaces and no external ornamentation.

*Description.*—General morphology as for genus. Some scales have two parallel sides longer than the other four sides, giving the scale a broadly rectangular shape. Corners rounded, with a thick rim surrounding the plate. Edge length 4.7–14.0  $\mu\text{m}$  (mean 8.8  $\mu\text{m}$ , standard deviation 2.5  $\mu\text{m}$ ); maximum diameter 25.8  $\mu\text{m}$  to 8.4  $\mu\text{m}$  (mean 17.2  $\mu\text{m}$ , standard deviation 5.5  $\mu\text{m}$ ),  $N=11$ . Thickness of plate, when measurable, ranges from 1–2  $\mu\text{m}$ . Gap between larger and smaller surfaces, where visible, 1–2  $\mu\text{m}$ .

*Etymology.*—In reference to the senior author's first mentor in paleontology, Dr. Warren Allmon.

*Types.*—Holotype YG#418.18 (Fig. 8.5) from sample T714-256 (SEM stub 256-g8), Neoproterozoic Mount Slipper locality, Fifteenmile Group, Yukon Territory.

*Material examined.*—Eight complete specimens, four partial specimens from meter 256.

*Occurrence.*—Fifteenmile Group, Mount Slipper, Section T714, Yukon Territory.

*Remarks.*—The fact that even-sided and rectangular forms are found in close proximity to each other suggests that they do not record different species but rather variations within a single population. In some specimens, the apparently thin internal surface seems to be degraded away, leaving behind only the rim (i.e., Fig. 13.4, top specimen). Specimens found individually or in clusters of two to three scales.

#### HEXACATILLUS RETETANTILLUS new species

Figure 8.7, 8.8

*Diagnosis.*—A species of *Hexacatillus* with a perforated basal surface.

*Description.*—Hexagonal plate with six relatively even sides. Scales perforated, with hexagonal pores defined by interwoven latticework. Corners rounded with a slightly raised rim surrounding plate. In some instances, rim appears to be broken away, indicating that the edge of the plate may rise up and curl over slightly to form the rim structure. Scale diameter 12  $\mu\text{m}$ , edge length 7.3  $\mu\text{m}$ ;  $N=8$ .

*Etymology.*—From the Latin *rete*, meaning net, and *tantillus*, meaning so small.

*Types.*—Holotype YG#418.20 (Fig. 8.7, 8.8) from sample T714-256 (SEM stub 256-g8), Neoproterozoic Mount Slipper locality, Fifteenmile Group, Yukon Territory.

*Material examined.*—Eight specimens, meter 256.

*Occurrence.*—Fifteenmile Group, Mount Slipper, Section T714, Yukon Territory.

*Remarks.*—Found in a cluster of eight to twelve scales. The rim of *H. retetantillus* appears less robust than that of *H. allmonii*.

#### Genus OSPERCAPATERA new genus

*Type species.*—*Ospercapatera awramikii* n. sp. by monotypy.

*Diagnosis.*—Muroolith form with solid central area and low rim. The rim, or lip, is constructed of rib-like struts at a right angle to the edge of the lip and covered with a thin sheeting.

*Etymology.*—Latin *os* for bone, *perca* for fish, and *patera* for shallow dish, in reference to the ribbed edges of the scales which are reminiscent of small fish bones.

*Remarks.*—No other taxa from the Fifteenmile assemblage display the fine rib-like struts seen in the lip of *Ospercapatera*.

#### OSPERCAPATERA AWRAMIKII new species

Figure 9.1–9.6

*Diagnosis.*—A species of *Ospercapatera* with maximum scale dimension of approximately 20  $\mu\text{m}$ .

*Description.*—Ovoid scales with imperforate central plate and a conspicuous rib or lip that folds over toward the plate center. Rim supported structurally by thin, regularly arranged struts that run perpendicular to edge. Scale length 22.8  $\mu\text{m}$ , width 18.3  $\mu\text{m}$ , ribbed lip width 4.2  $\mu\text{m}$ . Lip contains two lengths of ribs: longer ribs 4.2  $\mu\text{m}$  long, shorter ribs 700 nm long; all ribs 122 nm wide;  $N=1$ .

*Etymology.*—In honor of Dr. Stanley Awramik, who worked on the original samples of the Fifteenmile microfossils and aided our return to the locality.

*Types.*—Holotype YG#418.21 (Fig. 9.1, 9.2) from sample T714-312 (SEM stub 312-g4), Neoproterozoic Mount Slipper locality, Fifteenmile Group, Yukon Territory.

*Material examined.*—One complete specimen and three partial specimens, meter 312.

*Occurrence.*—Fifteenmile Group, Mount Slipper, Section T714, Yukon Territory.

*Remarks.*—Doubled muroolith form suggests that multiple plates interlocked together to form an outer covering to a cell. Only one complete specimen has been found, though numerous fragments of the rim were found in close proximity to the complete scale, suggesting damage and degradation of a larger aggregation of scales.

#### Genus PALEOMEGASQUAMA Allison and Hilgert, 1986

*Type species.*—*Paleomegasquama coccolithoides* Allison and Hilgert, 1986.

#### PALEOMEGASQUAMA ARCTOA new species

Figure 9.7–9.9

*Diagnosis.*—A species of *Paleomegasquama* with two surfaces connected by an inwardly curved surface.

*Description.*—Ovoid scale with two distinct flat oval surfaces separated by an inwardly curved surface. Placolith form. Distal flange extends farther out than proximal flange. Mean plate length, 19.6  $\mu\text{m}$  (minimum 7.3  $\mu\text{m}$ , maximum 30.8  $\mu\text{m}$ ); mean plate width, 15.5  $\mu\text{m}$  (minimum 5.8  $\mu\text{m}$ , maximum 26.3  $\mu\text{m}$ ); mean lip width, 3.1  $\mu\text{m}$  (minimum 1.3  $\mu\text{m}$ , maximum 4  $\mu\text{m}$ );  $N=6$ .

*Etymology.*—From the Latin *arctous* meaning “belonging to the bear,” with reference to an encounter with a grizzly bear at the Mount Slipper locality during sample collection.

*Types.*—Holotype YG#418.24 (Fig. 9.8) from sample T714-256 (SEM stub 256-g8), Neoproterozoic Mount Slipper locality, Fifteenmile Group, Yukon Territory.

*Material examined.*—Three specimens from meters 256, 272, 312.

*Occurrence.*—Fifteenmile Group, Mount Slipper, Section T714, Yukon Territory.

*Remarks.*—The ability to extract the specimen in three dimensions from limestone allows for a true picture of the specimen's morphology, which is often occluded in thin section. Placolith form suggests interlocking mechanism similar to that

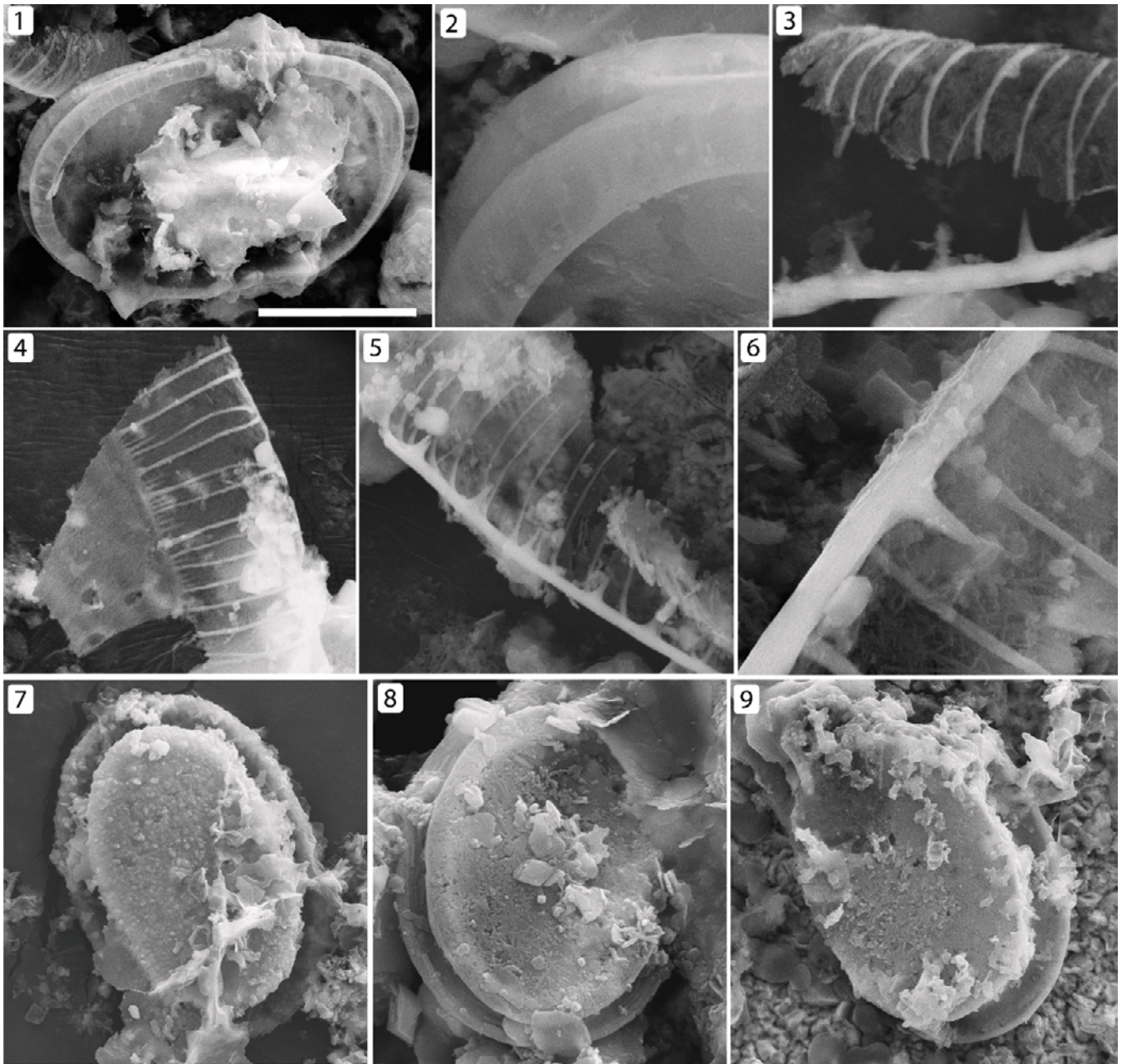


FIGURE 9—1–6, *Ospercapatera awramikii* n. gen n. sp.: 1, YG#418.21 (SEM stub 312-g4), complete specimen, central area obscured by matrix material; 2, detail of 1 showing a close up of the plate rim; 3, torn rim, visible in upper left hand corner of 1, showing struts detached from rim edge; 4, YG#418.22 (SEM stub 312-g4), partial damaged and detached rim and central plate area showing both types of rim struts; 5, concave side of detached rim in 4; 6, detail of struts attaching to rim edge in 4; 7–9, *Paleomegasquama arctoa* n. sp.: 7, YG#418.23 (SEM stub 256-g8); 8, YG#418.24 (SEM stub 272-g1); 9, YG#418.25 (256-g6). Scale bar is 10  $\mu$ m in 1; 2  $\mu$ m in 2; 3  $\mu$ m in 3; 3  $\mu$ m in 4; 3  $\mu$ m in 5; 2  $\mu$ m in 6; 10  $\mu$ m in 7; 4  $\mu$ m in 8; 10  $\mu$ m in 9.

seen in some coccoliths. This morphotype is given its own species name due to the difficulties of comparing specimens preserved in chert with those preserved in limestone. Specimens are found individually.

GENUS PALEOHEXADICTYON Allison and Hilgert, 1986

*Chilodictyon* Allison and Hilgert, 1986 (partim)

*Type species.*—*Paleohexadictyon litosum* ALLISON AND HILGERT, 1986.

*Diagnosis.*—Scale outline elliptical, slightly domed; margin simple or with raised rim. Pores arranged hexagonally, typically circular, uniform diameter across scale.

*Remarks.*—It is possible that some individuals assigned to

*Paleohexadictyon* originally had edge and pore node spines that have since been lost to diagenesis, in which case they would more properly be placed within the genus *Thorakidictyon*. However, it also appears that some scales truly have no spines or external ornamentations; thus, it is useful to retain the genus *Paleohexadictyon* for these specimens. See Table 1 and Table 2 for additional information on genus assignments.

PALEOHEXADICTYON LITOSUM Allison and Hilgert, 1986. emend.

Figure 10.1–10.5

1986 *Paleohexadictyon litosum* ALLISON AND HILGERT, p. 991, fig. 6.1, 6.2.

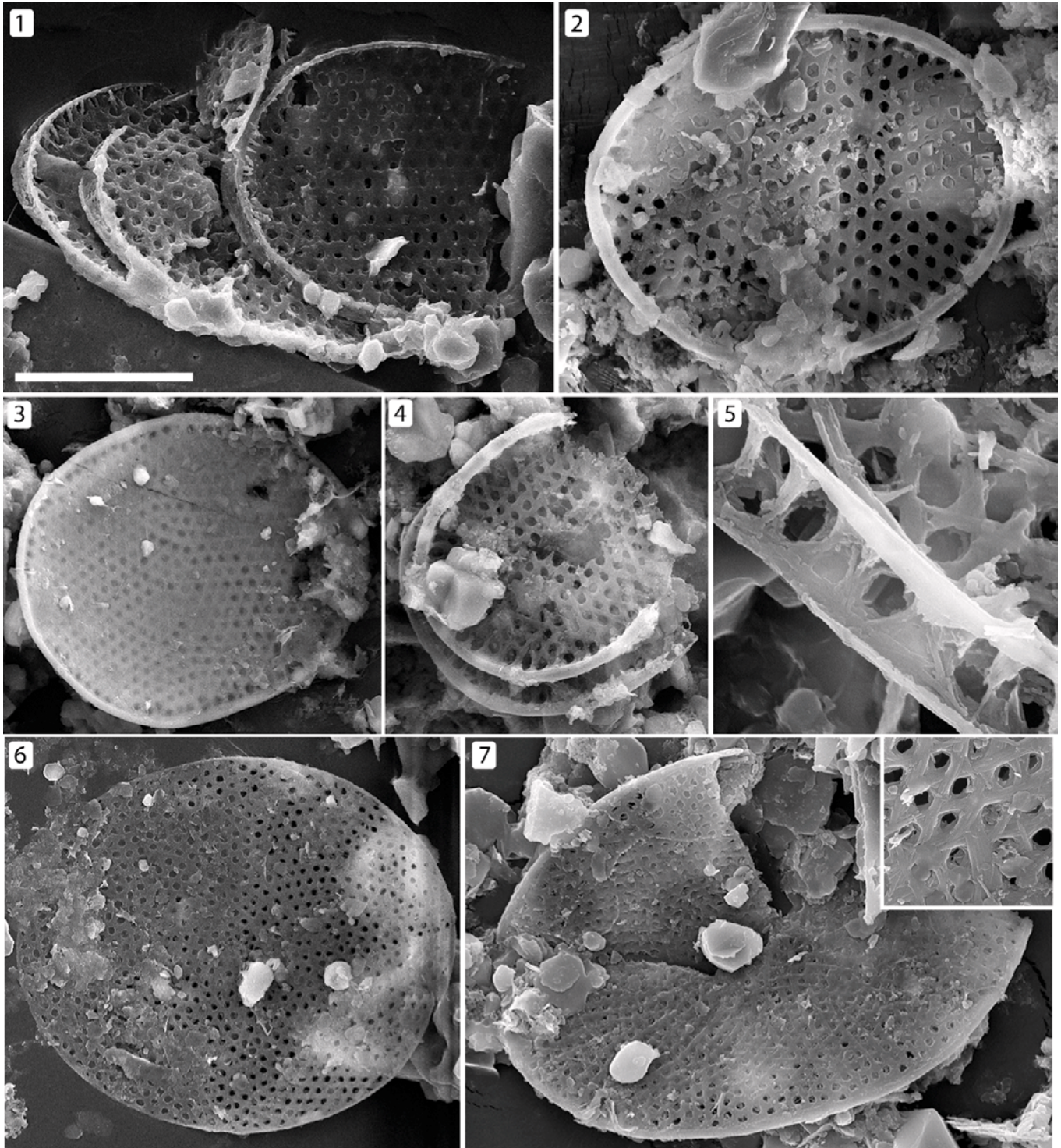


FIGURE 10—1–5, *Paleohexadictyon litosum* (Allison and Hilgert, 1986) emend. 1, YG#418.26 (SEM stub 312-12); 2, YG#418.27 (SEM stub 282-g4); 3, YG#418.28 (SEM stub 312-g2); 4, YG#418.29 (SEM stub 312-g2); 5, detail of 4 showing the fragmented plate edge; 6, 7, *Paleohexadictyon myriotrematum* (Allison and Hilgert, 1986): 6, YG#418.30 (SEM stub 282-g4); 7, YG#418.31 (SEM stub 282-g2), inset shows detail of hexagonal pore structure on plate surface. Scale bar is 15  $\mu\text{m}$  in 1; 9  $\mu\text{m}$  in 2; 14  $\mu\text{m}$  in 3; 14  $\mu\text{m}$  in 4; 3  $\mu\text{m}$  in 5; 14  $\mu\text{m}$  in 6; 5  $\mu\text{m}$  in 7.

1986 *Chilodictyon caliporum* ALLISON AND HILGERT, p. 996, fig. 7.6, 7.7.

1986 *Paleohexadictyon coroniforme* ALLISON AND HILGERT, p. 991, fig. 6.5.

1986 *Paleohexadictyon coroniforme* var. *tetragonum* ALLISON AND HILGERT, p. 991, fig. 6.4.

1986 *Paleohexadictyon coroniforme* var. *delicatum* Allison and Hilgert, 1986, p. 991, fig. 6.6.

*Diagnosis.*—Original: flat plate covered with 1 micron diameter pores, margin curled to form a tube-like ring around the scale. Emended: flat elliptical plates defined by hexagonal pores of approximately 1  $\mu\text{m}$  in diameter, containing an elevated rim, and lacking spines.

*Description.*—Elliptical plate with hexagonal pores close packed across the surface. Rim slightly elevated above the surface on one side of the plate. No spines on either surface. Mean maximum length, 29.2  $\mu\text{m}$  (maximum 47.6  $\mu\text{m}$ , minimum 17.5  $\mu\text{m}$ , standard deviation 7.9  $\mu\text{m}$ ); mean maximum width, 22.7  $\mu\text{m}$  (maximum 34.0  $\mu\text{m}$ , minimum 12.3  $\mu\text{m}$ , standard deviation 6.1  $\mu\text{m}$ ); mean pore diameter, 1.1  $\mu\text{m}$  (maximum 1.9  $\mu\text{m}$ , minimum 0.5  $\mu\text{m}$ , standard deviation 0.49  $\mu\text{m}$ );  $N=21$ .

*Material examined.*—Twenty-one samples from meters 272, 282, 312.

*Occurrence.*—Fifteenmile Group, Mount Slipper, Section T714, Yukon Territory.

*Remarks.*—The original description of this species contains discussion of a tube-like ring around the perimeter of the scales. It seems likely that this tube is actually the rounded raised rim of the plate, which may appear hollow and tubular when viewed in thin section. This species thus encompasses all specimens defined by hexagonal pores, containing an elevated rim, and lacking spines of any sort. Once we accept that the tube-like ring in the original description of *P. litosum* is a taphonomic artifact, the original description of *Chilodictyon caliporum* differs from that of *P. litosum* only by a description of differing pore sizes on different sides of the plate. We have observed no evidence of this in any specimen and believe that it may be due to the challenges of viewing such small-scale structures petrographically. Again, once we accept that the tube-like ring in the original description of *P. litosum* is a taphonomic artifact, the original descriptions of *Paleohexadictyon coroniforme*, *P. coroniforme* var. *tetragonum*, and *P. coroniforme* var. *delicatum* differ from *P. litosum* only through small variations in shape and size that we consider to be within the natural variability of the taxon. Scales of this taxa are often found individually but occasionally are found in stacks or clusters.

PALEOHEXADICTYON MYRIOTREMATUM Allison and Hilgert, 1986  
Figure 10.6, 10.7

*Description.*—Elliptical perforated scales with pores distributed in hexagonal close packing across surface. Similar to *P. litosum* but much smaller pore size. Mean maximum diameter 30.3  $\mu\text{m}$  (maximum 43.8  $\mu\text{m}$ , minimum, 19.4  $\mu\text{m}$ ); mean minimum diameter 22.2  $\mu\text{m}$  (maximum 28.4  $\mu\text{m}$ , minimum 16.4  $\mu\text{m}$ ); mean pore diameter 0.4  $\mu\text{m}$ ;  $N=5$ .

*Material examined.*—Five specimens, meters 312, 256, and 282.

*Occurrence.*—Fifteenmile Group, Mount Slipper, Section T714, Yukon Territory.

PALEOHEXADICTYON ALEXANDRAE new species  
Figure 11.5–11.7

*Diagnosis.*—A species of *Paleohexadictyon* with a smaller diameter than other species in the genus and pores larger than 1  $\mu\text{m}$  in diameter. Pores distributed irregularly across the scale surface and rim lacks spines.

*Description.*—Oval scale with basal surface defined by nearly circular or polygonal perforations. Planolith form with no raised rim, spines, or external ornamentation. Mean length, 19.8  $\mu\text{m}$  (maximum 23.3  $\mu\text{m}$ , minimum 17.5  $\mu\text{m}$ ); mean width 16  $\mu\text{m}$  (maximum 17.9  $\mu\text{m}$ , minimum 15.1  $\mu\text{m}$ ); mean pore diameter, 1.6  $\mu\text{m}$ ;  $N=3$ .

*Types.*—Holotype YG#418.36 (Fig. 11.5) from sample T714-272 (SEM stub 272-g1), Neoproterozoic Mount Slipper locality, Fifteenmile Group, Yukon Territory.

*Etymology.*—In honor of one of the first author's mentors in geology, Dr. Alexandra Moore.

*Material examined.*—Three specimens from meter 272.

*Occurrence.*—Fifteenmile Group, Mount Slipper, Section T714, meter 272, Yukon Territory.

*Remarks.*—This distinctive population is the only species of

*Paleohexadictyon* not described in Allison and Hilgert (1986). It is only known from macerated samples. Specimens are found individually.

Genus PALEOScutULA new genus

*Type species.*—*Paleoscutula inornata* n. sp.

*Other species.*—*Paleoscutula serrata* n. sp., *Paleoscutula convocationis* n. sp.

*Diagnosis.*—Flat square plate with sloping rim. Planolith form, with rim only slightly raised over the plane of central area. Central area solid, without any reticulation.

*Etymology.*—From the Latin *scutula*, meaning a square shaped plate, and *paleo*, meaning ancient.

*Remarks.*—This genus has only been found in macerated material.

PALEOScutULA INORNATA new species  
Figure 11.3, 11.4

*Diagnosis.*—A species of *Paleoscutula* with no apparent external ornamentation.

*Description.*—Flat solid square shaped plate with slightly raised rim. No other external features. Planolith form with rim only very slightly raised over the plane of the central area. Maximum diameter of plate 10.8  $\mu\text{m}$ ; rim width, 0.6  $\mu\text{m}$ ;  $N=3$ .

*Etymology.*—From the Latin *inornata*, meaning unornamented.

*Types.*—Holotype YG#418.34 (Fig. 11.3, 11.4) from sample T714-252 (SEM stub 252-g2), Neoproterozoic Mount Slipper locality, Fifteenmile Group, Yukon Territory.

*Material examined.*—Three specimens, meter 252.

*Occurrence.*—Fifteenmile Group, Mount Slipper, Section T714, Yukon Territory.

*Remarks.*—Scales found only as single specimens within macerated material.

PALEOScutULA CONVOCATIONIS new species  
Figure 11.1, 11.2

*Diagnosis.*—Species of *Paleoscutula* with a single prominent circular to sub-circular ring arising from one side of the plate.

*Description.*—Solid flat square shaped plate with slightly sloping rim. Planolith form with rim only slightly raised over the plane of the central area. Distinct singular circular to sub-circular ring on one side of the plate. The ring rises 1 to 2  $\mu\text{m}$  above the surface of the plate and covers almost the entire area of the square plate surface. Maximum length of plate 9  $\mu\text{m}$ ; maximum diameter of ring 6  $\mu\text{m}$ ; thickness of plate rim 1–2  $\mu\text{m}$ ;  $N=2$ .

*Etymology.*—From the Latin *convocatio* meaning calling together or convocation, in reference to the specimens' striking similarity to a commencement mortarboard.

*Types.*—Holotype YG#418.32 (Fig. 11.1) from sample T714-256 (SEM stub 256-g8), Neoproterozoic Mount Slipper locality, Fifteenmile Group, Yukon Territory.

*Material examined.*—Two specimens from meter 256.

*Occurrence.*—Fifteenmile Group, Mount Slipper, Section T714, Yukon Territory.

*Remarks.*—Scales found only as single specimens within macerated material. The central ring is not always perfectly circular.

PALEOScutULA SERRATA new species  
Figure 12

*Diagnosis.*—Species of *Paleoscutula* with multiple small spines lining the rim.

*Description.*—Solid flat square plate with flattened rim. Planolith form with rim only slightly raised over the plane of the central area. Rim edged with small blunt spines. Spines, clustered in groups of three along the edge of the plate rim, consist of bundles of easily visible apatite fibers. Maximum dimension of plate 17.2  $\mu\text{m}$ , mean spine length 0.6  $\mu\text{m}$ , plate rim thickness 1.5  $\mu\text{m}$ ;  $N=1$ .

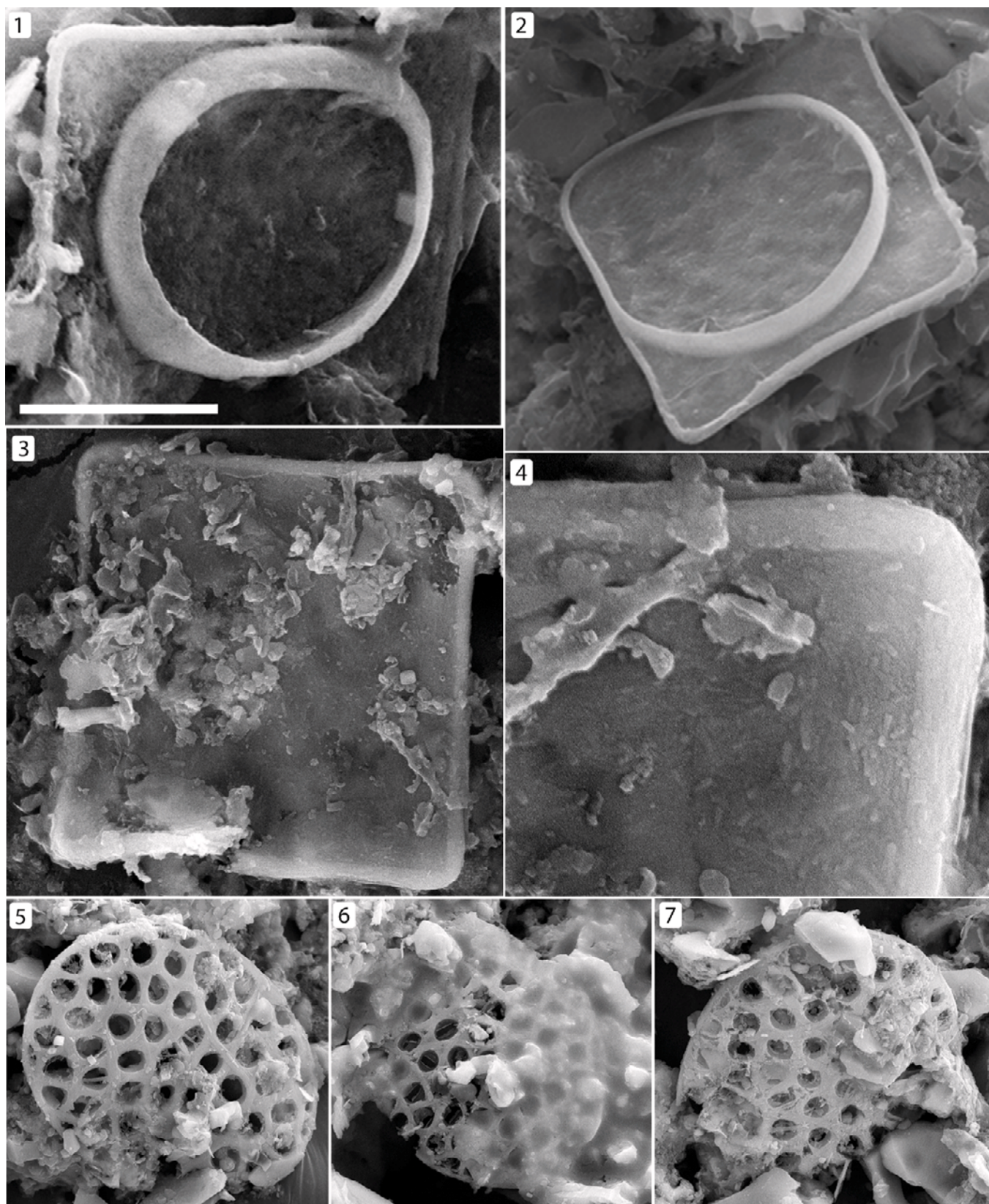


FIGURE 11—1, 2, *Paleoscutula convocationis* n. gen. n. sp.: 1, YG#418.32 (SEM stub 256-g8); 2, YG#418.33 (SEM stub 256-g8); 3, 4, *Paleoscutula inornata* n. gen. n. sp.: 3, YG#418.34 (SEM stub 252-g2); 4, detail of edge corner of 3; 5–7, *Paleohexadictyon alexandrae* n. sp.: 5, YG#418.36 (SEM stub 272-g1); 6, YG#418.37 (SEM stub 272-g1); 7, YG#418.38 (SEM stub 272-g2). Scale bar is 6  $\mu\text{m}$  in 1; 5  $\mu\text{m}$  in 2; 4  $\mu\text{m}$  in 3; 2  $\mu\text{m}$  in 4; 9  $\mu\text{m}$  in 5, 6, 7.

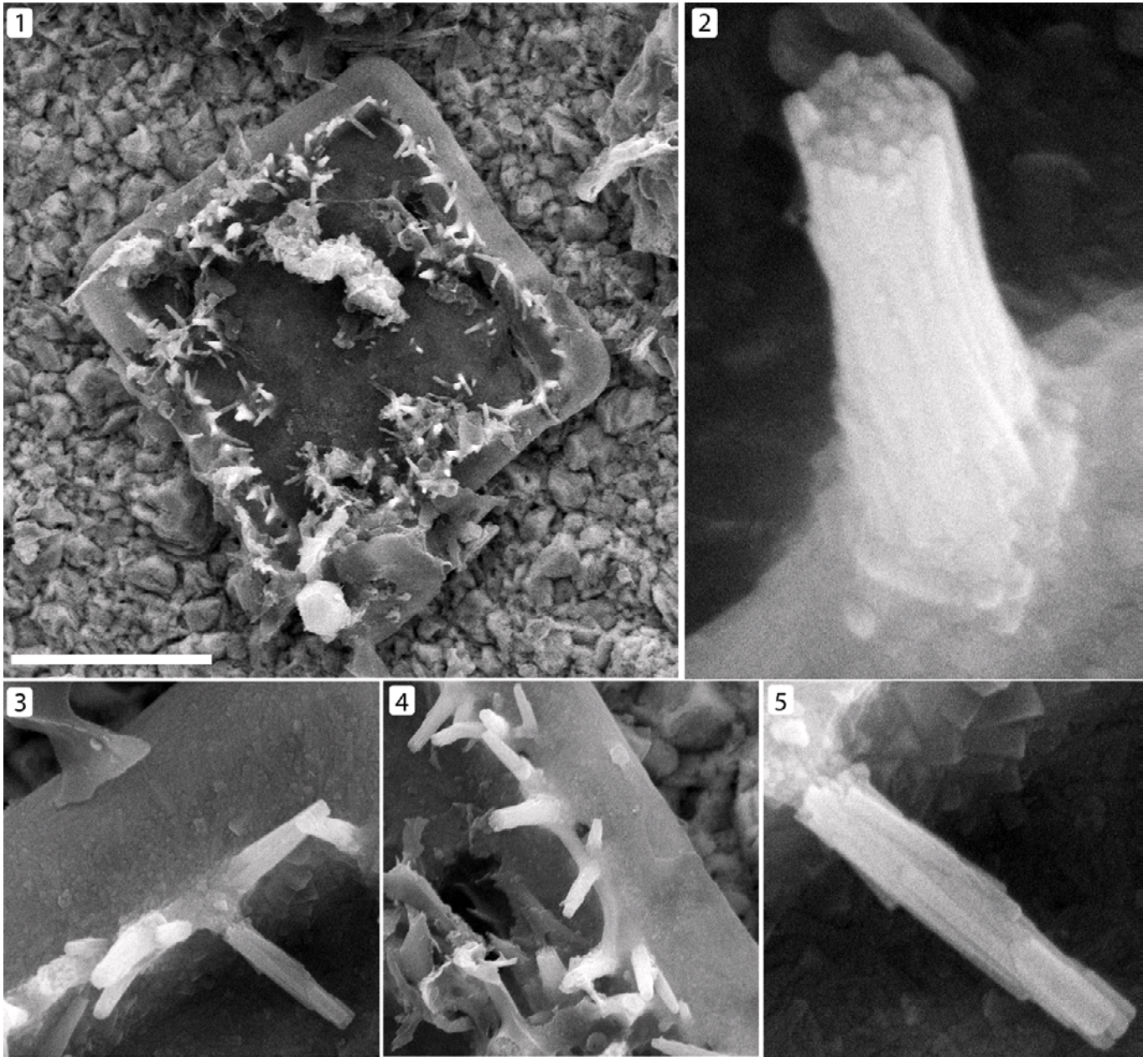


FIGURE 12—*Paleoscutula serrata* n. gen n. sp. YG#418.39 (SEM stub 256-g8). 1, full scale; 2, detail of a single edge spine showing bundled apatite fibers; 3, detail of edge spines showing clustering of spines; 4, detail of edge spines showing narrow spacing between spines and changing angles of spines relative to scale rim; 5, detail of edge spine showing bundled apatite fibers running the length of the spine. Scale bar is 8  $\mu\text{m}$  for 1; 300 nm in 2; 2  $\mu\text{m}$  in 3; 3  $\mu\text{m}$  in 4; 800 nm in 5.

*Types*.—Holotype YG#418.39 (Fig. 12.1–12.5) from sample T714-256 (SEM stub 256-g8), Neoproterozoic Mount Slipper locality, Fifteenmile Group, Yukon Territory.

*Etymology*.—From the Latin *serrata* meaning toothed, in reference to the tooth-like spines projecting from the rim.

*Material examined*.—One specimen from meter 256.

*Occurrence*.—Fifteenmile Group, Mount Slipper, Section T714, Yukon Territory.

*Remarks*.—Only one specimen found, in isolation. However, the three taxa of imperforated square scales differ markedly in their type and degree of ornamentation and are thus easily distinguished.

Genus PETASISQUAMA Allison and Hilgert, 1986

*Type species*.—*Petasisquama alta* Allison and Hilgert, 1986.

#### PETASISQUAMA PETASUS new species

##### Figure 13

*Diagnosis*.—A species of *Petasisquama* with a distinct wide and upward-curving rim.

*Description*.—Imperforate hat-shaped form with wide rim that curves slightly upwards. Top of the ‘hat’ is flat, with rounded edges and represents the only planar surface. Sides are slightly sub-parallel, and generally perpendicular to the plane of the lip with a concave curved profile. High magnification reveals fibrous striations on concave side walls. Placolith form, distal flange extends farther than proximal flange. Width of proximal surface 15.1  $\mu\text{m}$ ; length of proximal surface 21.5  $\mu\text{m}$ ; lip flange width 2.6  $\mu\text{m}$ ; height from proximal surface to distal surface 2  $\mu\text{m}$ ; N=2.

*Etymology*.—From the Latin *petasus*, for a broad-brimmed hat.

*Types*.—Holotype YG#418.40 (Fig. 13.1, 13.2) from sample

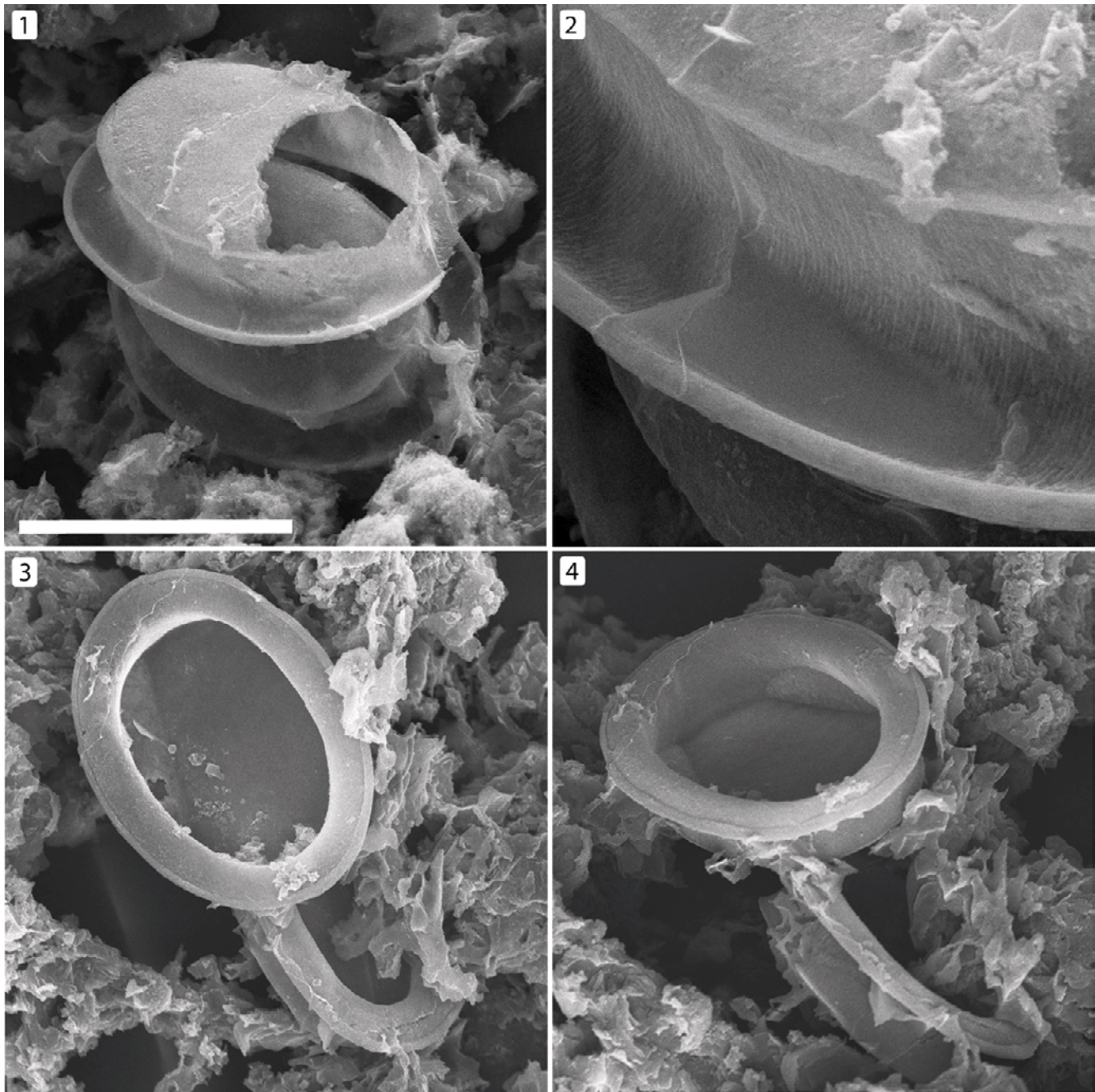


FIGURE 13—*Petasisquama petasus* n. sp. YG#418.40 (SEM stub 256-g8). 1, view showing proximal surface with damage; 2, detail of side wall in 1 showing striations; 3, distal surface of YG#418.41 (SEM stub 256-g8); 4, distal surface and side walls of 3. Scale bar is 15  $\mu$ m in 1; 8  $\mu$ m in 2; 16  $\mu$ m in 3; 17  $\mu$ m in 4.

T714-256 (SEM stub 256-g8), Neoproterozoic Mount Slipper locality, Fifteenmile Group, Yukon Territory.

*Material examined*.—Two specimens from meter 256.

*Occurrence*.—Fifteenmile Group, Mount Slipper, Section T714, Yukon Territory.

*Remarks*.—Specimens found in groups of two scales. Bottom surface of scale is very robust as compared to other ovoid taxa. Damage to the scale seen in Figure 13.1 indicates a brittle composition.

#### Genus QUADRIRETICULUM new genus

*Type species*.—*Quadrireticulum allisoniae* n. sp.

*Other species*.—*Quadrireticulum palmaspinosum* n. sp.

*Diagnosis*.—Flat square plates. Scales perforated, with hexag-

onal pores defining the surface. Scales often arranged in clusters in macerated specimens. Planolith form with low thickened rim rising slightly over the central area.

*Etymology*.—From the Latin *quadri*, meaning four, and *reticulum*, meaning net.

*Remarks*.—The surface perforations seen in this genus are very similar to those seen in other Fifteenmile genera such as *Characodictyon* and *Paleohexadictyon*. This genus is only observed in macerated material.

#### QUADRIRETICULUM ALLISONIAE new species

Figure 14.3, 14.4

*Diagnosis*.—A species of *Quadrireticulum* with no external ornamentation.



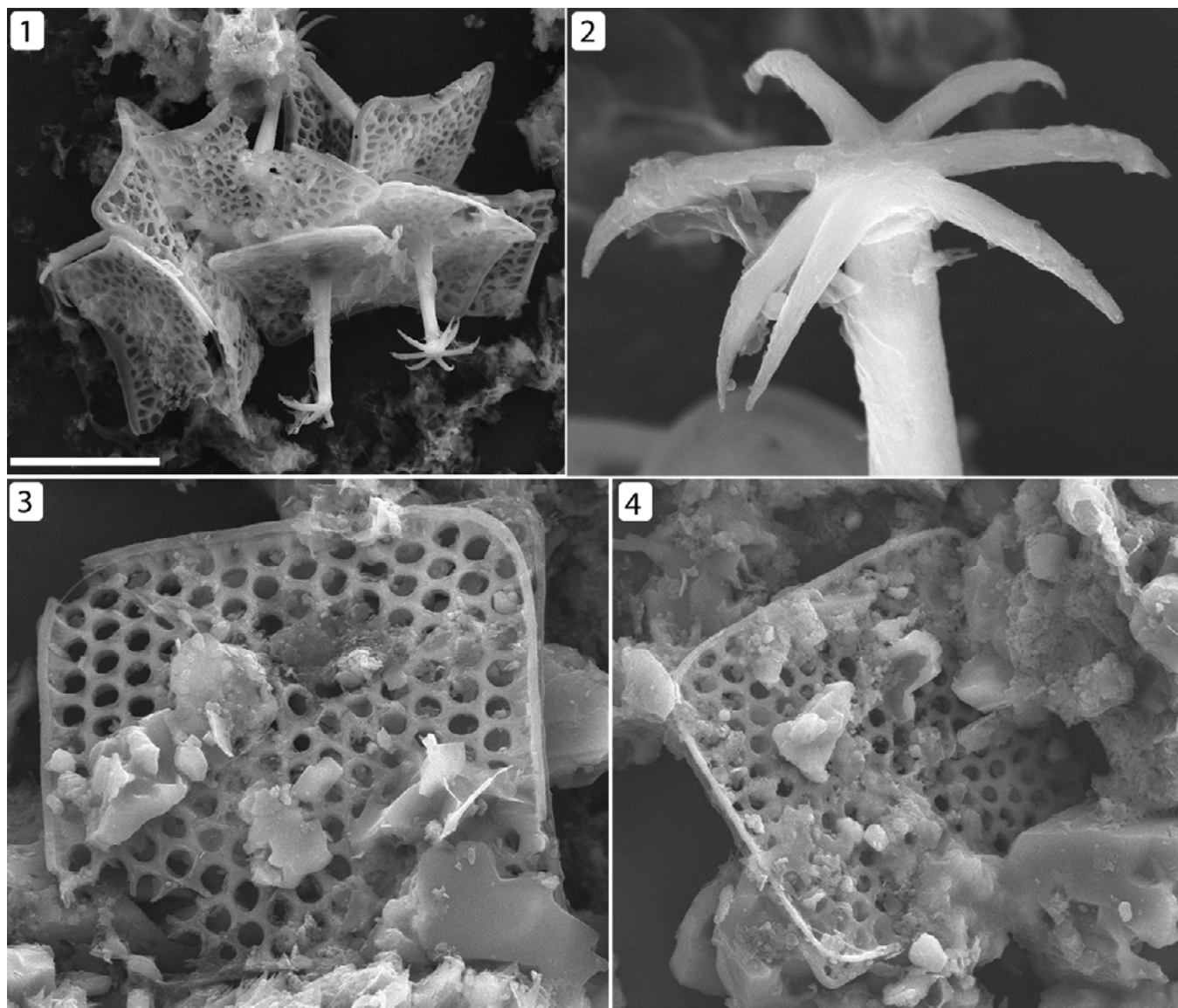


FIGURE 14—1, 2, *Quadrireticulum palmaspinosum* n. gen n. sp. 1, YG#418.42 (SEM stub 256-g6), cluster of scales; 2, detail of one scale from cluster shown in 1; 3, 4, *Quadrireticulum allisoniae* n. gen n. sp.; 3, YG#418.43 (SEM stub 272-g1); 4, YG#418.44 (SEM stub 272-g1). Scale bar is 14  $\mu\text{m}$  in 1; 3  $\mu\text{m}$  in 2; 7  $\mu\text{m}$  in 3; 8  $\mu\text{m}$  in 4.

*Description.*—General morphology as for genus. No visible spines on either surface. Mean diameter 24.5  $\mu\text{m}$ ; mean pore size 0.7  $\mu\text{m}$ ; lip width 0.3–0.6  $\mu\text{m}$ ; N=4.

*Etymology.*—In memory of Dr. Carol Allison who discovered the Fifteenmile scale microfossils.

*Types.*—Holotype YG#418.43 (Fig. 14.3) from sample T714-272 (SEM stub 272-g1), Neoproterozoic Mount Slipper locality, Fifteenmile Group, Yukon Territory.

*Material examined.*—Four specimens from meter 272.

*Occurrence.*—Fifteenmile Group, Mount Slipper, Section T714, Yukon Territory.

*Remarks.*—Similar to *Quadrireticulum palmaspinosum* but lacking a central spine. Some minor variation in pore diameter between specimens. In some instances, the two rims differ in shape where one forms a more rounded corner and the other is closer to a right angle. Unlike *Q. palmaspinosum*, this species is only found as single scales within macerated material.

#### QUADRIRETICULUM PALMASPINOSUM new species

Figure 14.1, 14.2

*Diagnosis.*—A species of *Quadrireticulum* with a single prominent spine that extends on one side from the center of the plate.

*Description.*—General plate morphology as for genus. Single spine extending at a right angle from the center of one side of the flat plate and terminating in anchor-like structure. Anchor has seven spines that radiate out in a slightly uneven pattern from anchor terminus. Spines curve gently downwards from base to tip. Edge length 4.7  $\mu\text{m}$ , maximum diameter 9–13  $\mu\text{m}$ , plate thickness 0.5–1  $\mu\text{m}$ ; pore diameter 1  $\mu\text{m}$ , central spine length 8.8  $\mu\text{m}$ , central spine width 1.5  $\mu\text{m}$ , anchor point length, 3.5  $\mu\text{m}$ ; N=7.

*Etymology.*—From the Latin *palma*, for the palm tree, and *spinus*, meaning spined.

*Types.*—Holotype YG#418.42 (Fig. 14.1, 14.2) from sample T714-256 (SEM stub 256-g6), Neoproterozoic Mount Slipper locality, Fifteenmile Group, Yukon Territory.

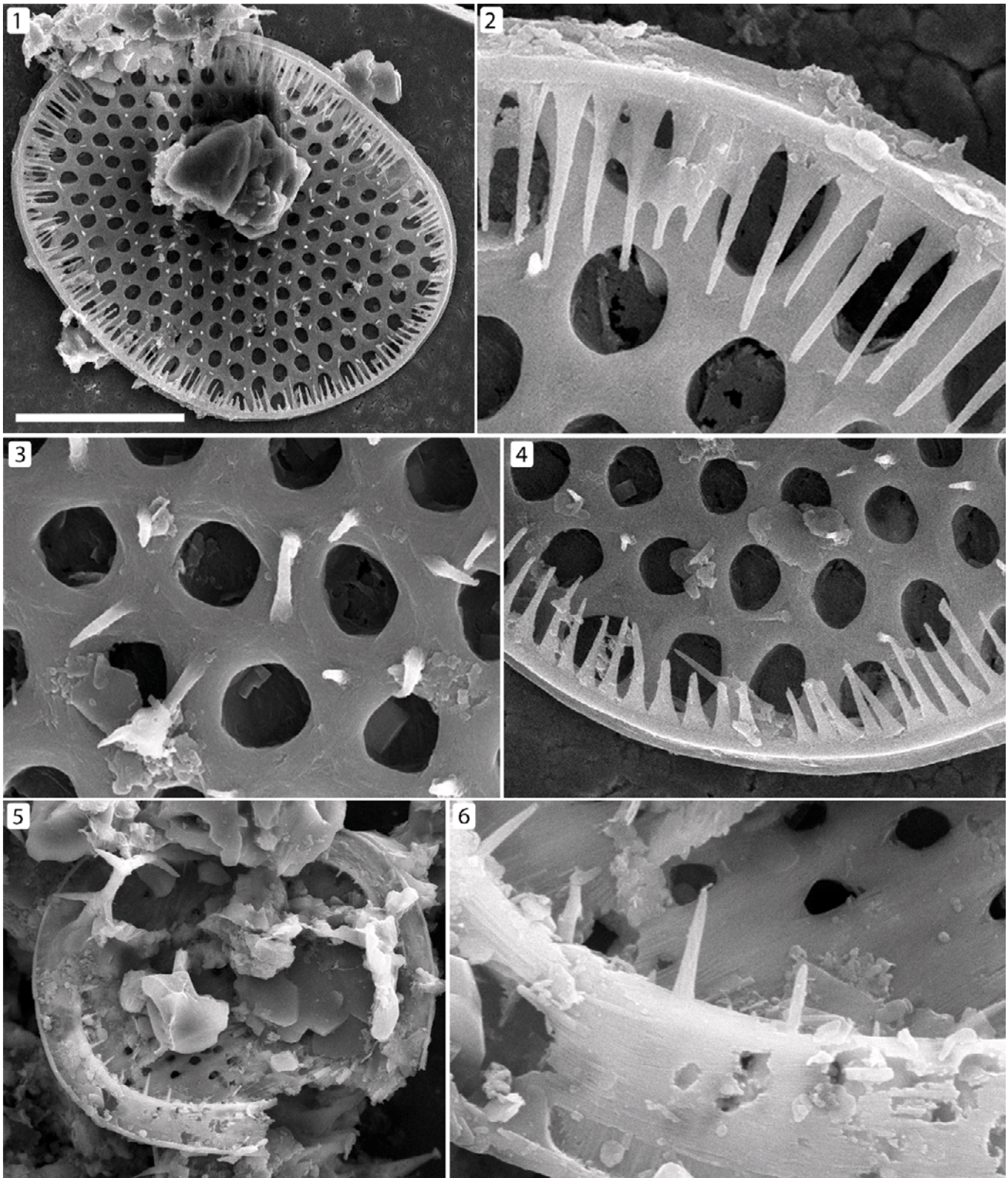


FIGURE 15—Genus *Thorakidictyon* n. gen. 1–4, *Thorakidictyon myriocanthum* (Allison and Hilgert, 1986) n. comb.: 1, YG#418.45 (SEM stub 312-stub12), full scale showing rim edge spines; 2, detail of edge spines in 1; 3, detail of pore intersection spines in 1; 4, detail of edge spines and pore intersection spines in 1; 5, 6, *Thorakidictyon circireticulum* n. gen n. sp.: 5, YG#418.46 (SEM stub 272-g2); 6, detail of 5 showing edge spines. Scale bar is 14  $\mu$ m in 1; 2  $\mu$ m in 2; 2  $\mu$ m in 3; 5  $\mu$ m in 4; 15  $\mu$ m in 5; 3  $\mu$ m in 6.

*Material examined.*—Seven specimens, meter 256.

*Occurrence.*—Fifteenmile Group, Mount Slipper, Section T714, Yukon Territory.

*Remarks.*—Specimens found in clusters, suggesting their placement around a larger central cell body. Similar overall to *Characodictyon skolopium* except that plate outline is square rather than elliptical. The hexagonal network patterning on the basal surface species appears less geometric than in other species with hexagonal pores; i.e., there are fewer consistently regular hexagonal pores and more irregularly shaped pores.

#### Genus THORAKIDICTYON new genus

*Type species.*—*Thorakidictyon myriocanthum* new comb.

*Other species.*—*Thorakidictyon circireticulum* n. sp.

*Diagnosis.*—Plate with pores arranged in hexagonal close-packing. Rim slightly elevated above the surface of one side of the plate. Spines present around the edge of the scale. Spines also present on struts that define pore intersections.

*Etymology.*—From the Greek *thorakisi*, meaning armor, with reference to the spines, and *dictyon*, from the Greek meaning net-like.

*Remarks.*—As we have concluded that the original type species of *Chilodictyon*, *C. caliporum*, actually belongs to the genus *Paleohexadictyon*, the species once included within *Chilodictyon* now require a new genus. We propose the name *Thorakidictyon*.

Poor preservation often destroys pore intersection and edge spines, making the distinction between *Thorakidictyon* and *Paleohexadictyon* challenging. There is little risk in confusing *Thorakidictyon* with *Characodictyon* as it is much more difficult to remove all evidence of the latter's central spine. See Table 1 and Table 2 for additional information on genus assignments.

#### THORAKIDICTYON MYRIOCANTHUM

(Allison and Hilgert, 1986)

Figure 15.1–15.4

1986 *Chilodictyon myriocanthum* ALLISON AND HILGERT, p. 996, fig. 8.1–8.3.

1986 *Chilodictyon caliporum* var. *striomarginatum* ALLISON AND HILGERT, p. 996, fig. 7.8, 7.9.

*Holotype.*—*Chilodictyon myriocanthum* ALLISON AND HILGERT, 1986, fig. 8.3.

*Diagnosis.*—A species of *Thorakidictyon* with numerous uniform acicular spines closely packed along scale rim.

*Description.*—Oval plate with surface defined by hexagonal pores. On one surface, spines are present in two different arrangements. Spines present around edge of scale, facing inwards at almost right angle so that edge spines are nearly parallel to plate surface. Spines also present at intersection of hexagonal pores, each intersection spine extending upward at a right angle to plate surface. Mean length 35  $\mu\text{m}$  (maximum 49.6  $\mu\text{m}$ , minimum 17.5  $\mu\text{m}$ , standard deviation 10.4  $\mu\text{m}$ ); mean width 26.9  $\mu\text{m}$  (maximum 36.6  $\mu\text{m}$ , minimum 16.5  $\mu\text{m}$ , standard deviation 7  $\mu\text{m}$ ); mean pore diameter 1.1  $\mu\text{m}$ ; pore intersection spine length 0.8–1.5  $\mu\text{m}$ ; mean edge spine length 2.2  $\mu\text{m}$  (maximum 3  $\mu\text{m}$ , minimum 1.1  $\mu\text{m}$ , standard deviation 0.7  $\mu\text{m}$ ); N=10.

*Types.*—Holotype YG#418.45 (Fig. 15.1–15.4) from sample T714–312 (SEM stub 312–stub12), Neoproterozoic Mount Slipper locality, Fifteenmile Group, Yukon Territory.

*Material examined.*—Ten samples from meter 312.

*Occurrence.*—Fifteenmile Group, Mount Slipper, Section T714, Yukon Territory.

*Remarks.*—Poor preservation often destroys the pore intersection and edge spines, making the distinction between *Thorakidictyon* and *Paleohexadictyon* challenging. However, in limestone-hosted specimens all specimens with pore intersection spines also have rim edge spines on one surface. Some samples show edge spines without pore node spines but we believe this to

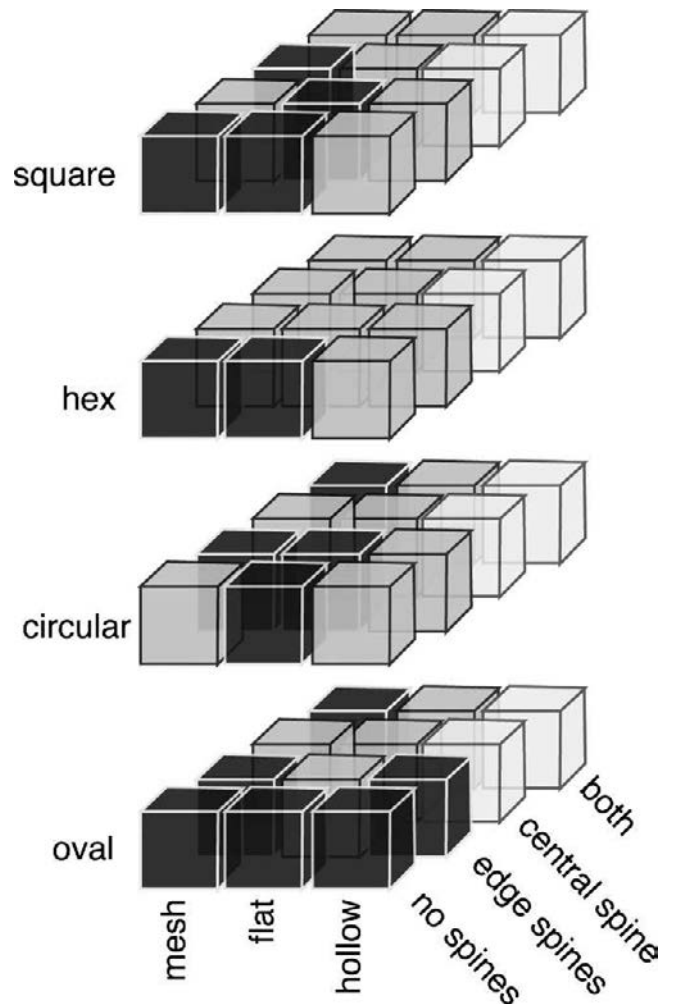


FIGURE 16—Discrete morphospace of select ASM taxon characters: white='impossible' (i.e., hollow taxa cannot have a central spine); grey=not present; black=present in at least one taxon; 'Both'=both a central spine and edge spines.

be due to varying diagenetic sensitivity. See Table 2 for additional information on genus assignments. Scales often found individually but occasionally are found in stacks or clusters.

#### THORAKIDICTYON CIRCIRETICULUM new species

Figure 15.5, 15.6

*Diagnosis.*—A species of *Thorakidictyon* with a circular outline and low spine density along rim.

*Description.*—Scale with circular to sub-circular outline. Basal surface of scales perforate in regular hexagonal pattern. Wide, raised marginal rim. Spines present at relatively low density on inner edge of rim, oriented toward plate center. Scale dimensions 30.1  $\mu\text{m}$  by 24.4  $\mu\text{m}$ ; rim width, 2.9  $\mu\text{m}$ ; spine length, 1.5  $\mu\text{m}$ ; N=1.

*Etymology.*—Latin *circi* for ring and *reticulum* for netted.

*Types.*—Holotype YG#418.46 (Fig. 15.5, 15.6) from sample T714-272 (SEM stub 272-g2), Neoproterozoic Mount Slipper locality, Fifteenmile Group, Yukon Territory.

*Material examined.*—One specimen from meter 272.

*Occurrence.*—Fifteenmile Group, Mount Slipper, Section T714, Yukon Territory.

*Remarks.*—Unlike *Thorakidictyon myriocanthum*, the spines of *T. circireticulum* protrude only from the very inner edge of the rim which is significantly wider than in *T. myriocanthum*. While

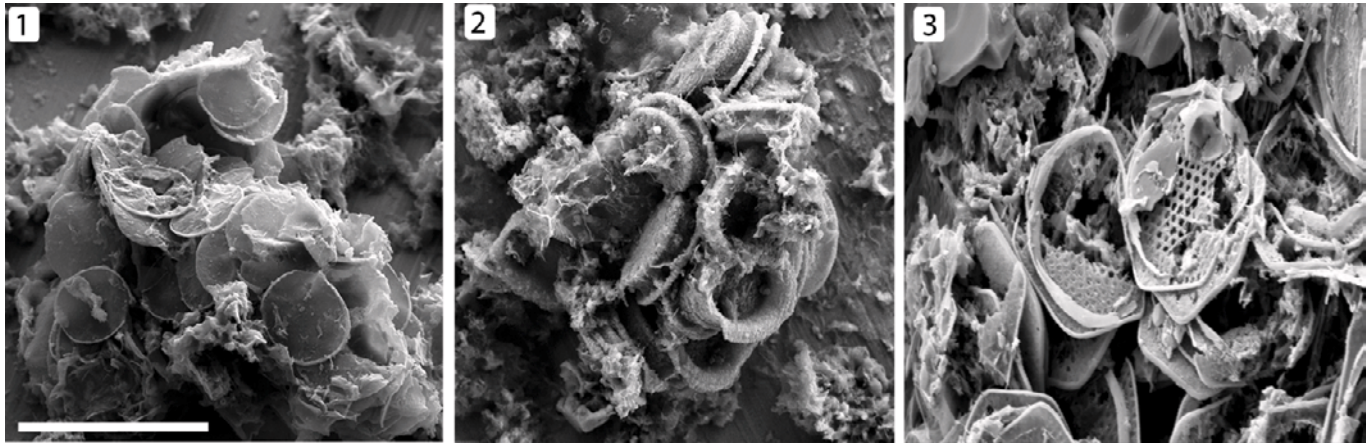


FIGURE 17—Scanning electron microscope (SEM) photomicrographs of scale clusters. 1, *Archaoxybaphon polykeramoides* emend; 2, *Paleomegasquama arctoa* n. sp.; 3, *Hexareticulum retetantillus* n. gen. n. sp. Scale bar in 1 is 30  $\mu\text{m}$ ; 50  $\mu\text{m}$  in 2; and 20  $\mu\text{m}$  in 3.

the specimen is not entirely round, it is to a much greater degree than any examine specimens of *T. myriocanthum*. Only one isolated specimen found.

#### TAXONOMIC DIVERSITY

The Fifteenmile specimens vary along three principal axes of morphology (Fig. 16): overall shape, basal surface, and spines. In overall shape, scales are circular, elliptical, square, or hexagonal in outline. The distribution of shapes among samples is not consistent with some horizons containing all four shape types and others containing only a single shape. (The horizons with single shape types [252m and 282m] also have the lowest number of recovered samples, so this pattern may be an artifact of sampling.) Overall, ovoid forms dominate the assemblage.

Basal surface variation includes central surfaces are either solid, display hexagonally close-packed pores defined by mesh-like network of interwoven struts, or are absent. Strut patterns are consistent across all genera that contain them.

Spines vary as many morphotypes have a central boss-like spine and/or fine tooth-like spines that rim scale edges.

Figure 16 shows a matrix of these characters. Note that all four shape categories contain at least one population with a mesh surface; square and oval scales display all possible combinations of surface and spine types, whereas hexagonal taxa do not display spines at all. In addition, only mesh-surfaced taxa have central spines, and only oval shaped forms lack a central surface. In general, morphological characters present in the fossils are discrete, indicating multiple unique and identifiable species, as opposed to polymorphisms within a smaller number of taxa. Scale aggregations, visible both in thin section (Allison and Hilgert, 1986) and in maceration (Fig. 17), presumably represent sets of scales formed by an individual organism. These contain only a single type of scale, increasing confidence in the relationship between scale taxonomy and original biological diversity. We note, however, that some modern protists can fashion distinct scale morphologies at different points in their life cycle (Lewis and McCourt, 2004). Thus, the possibility exists that more than one scale morphotype was produced by a single biological species.

Allison and Hilgert (1986) used scale shape, the solid or perforated nature of the central plate, and the presence or absence of spines as the primary characters for taxonomic classification. We follow this precedent here, knowing that the

resulting assignment of scale populations to different genera may be more practical than biological. For example, considering the perforate or solid nature of the plate as a primary character would result in a somewhat different classification at the genus level but the same number of recognized form species.

On the basis of these features, the Mount Slipper section of the Fifteenmile Group contains 38 species in 22 genera. Seventeen of these species and six genera have been found only in carbonate macerates so are newly described here. An additional six species have been found in both chert thin section and carbonate macerates, and 15 species have so far only been found in chert as documented in Allison and Hilgert (1986). Allison and Hilgert (1986) formally subdivided a number of species into varieties but we have not continued that practice here; see systematic paleontology section for additional details. We have emended taxa originally described in Allison and Hilgert (1986) on the basis of additional morphological detail only available from the carbonate-hosted specimens. Table 1 lists all taxa documented from both Fifteenmile carbonates and cherts.

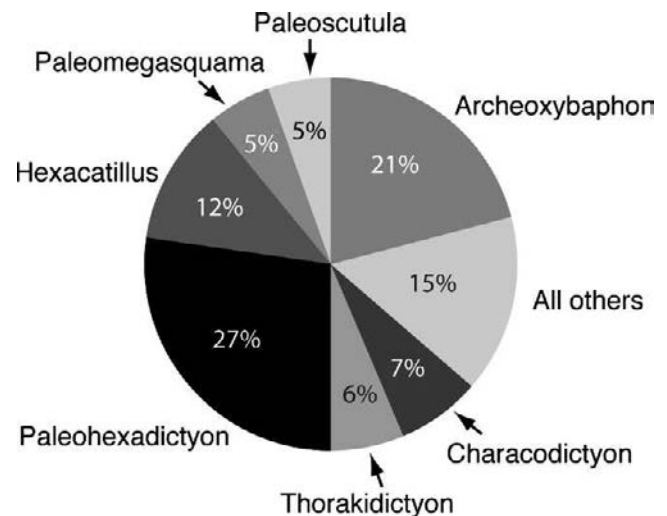


FIGURE 18—Relative distribution of genera in all samples, N=110.

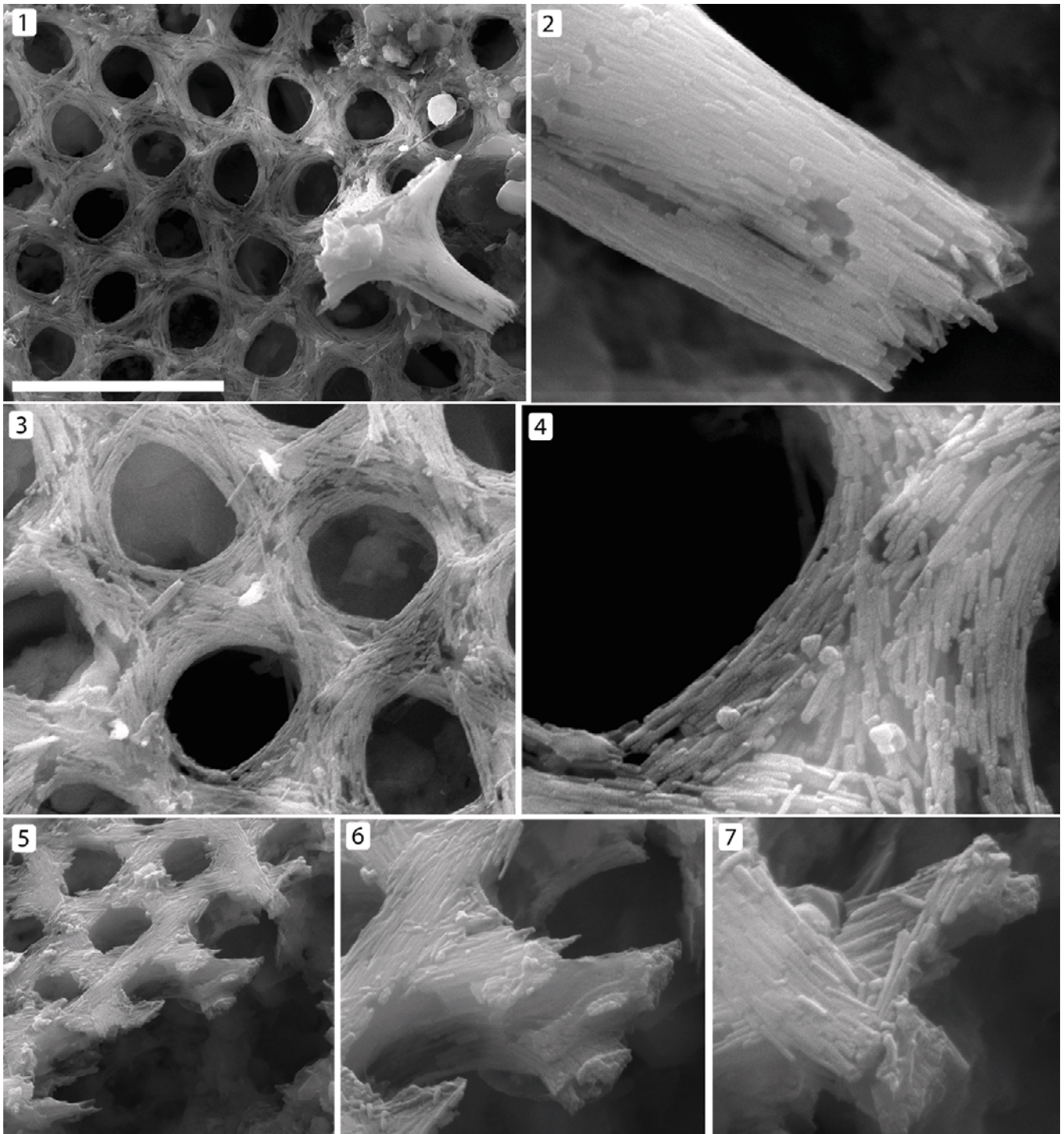


FIGURE 19—SEM photomicrographs of the microstructure of *Characodictyon skolopium*. 1, top-down view of reticulate scale surface and damaged anchor/spine assembly; 2, detail of one of the anchor spines showing distinct apatite fibers running parallel to the surface; 3, detail of hexagonal pores that make up the surface of the scale, showing interwoven bundles of apatite fibers; 4, detail of one of the struts constructing the sides of the hexagonal pores showing variation in the length and arrangement of the apatite fibers; 5, 6, 7, detail showing increasing magnification from left to right, of a fractured specimen demonstrating the overlapping and interwoven habit of the apatite fibers that make up the struts of the surface of the fossil. Scale bar is 4  $\mu\text{m}$  in 1; 1.2  $\mu\text{m}$  in 2; 2.5  $\mu\text{m}$  in 3; 1  $\mu\text{m}$  in 4; 4  $\mu\text{m}$  in 5; 2  $\mu\text{m}$  in 6; 1.5  $\mu\text{m}$  in 7.

Species diversity within individual sample horizons ranges from three to 10. The most abundant genera are *Paleohexadictyon* and *Archeoxybaphon*, comprising 27% and 21% of all individuals, respectively (Fig. 18). The dominance of *Archeoxybaphon* may be due to the fact that this genus is

morphologically simple and thus difficult to sub-divide based on the characters used here for taxonomic differentiation.

Taxon distribution is not uniform throughout the fossiliferous section. For example, square and hexagonal taxa are found only in the lowest two fossiliferous horizons and taxa with spines are

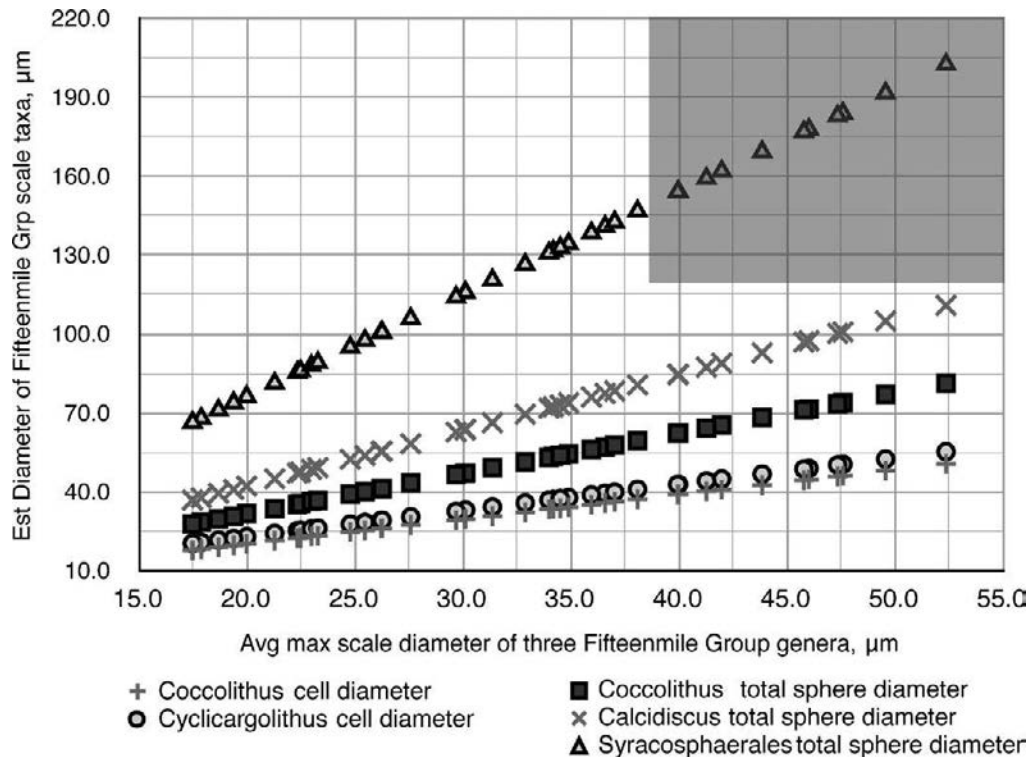


FIGURE 20—Estimated total sphere (cell plus scales) and cell diameter (total sphere minus scales) reconstructions based on the average diameter of three taxa (*Characodictyon skolopium*, *Thorakidictyon myriocanthum* n. comb., and *Paleohexadictyon litosum* emend.) using linear relationships between single scale diameter and total sphere and cell diameter for four coccolithophore genera, derived from Henderiks (2008). Each data point represents one fossil specimen; the x-axis value is the diameter of each fossil specimen; the y-axis value is the inferred diameter of the total sphere or cell diameter of the fossil organism based on the scale size to total sphere or cell diameter relationship for the corresponding coccolithophore taxon; the gray square represents unlikely space filled by a very large total sphere made up of many very large plates.

never found in the lowest horizon (Fig. 1.3). At present, we cannot judge whether this distribution primarily reflects evolutionary turnover or environmental preference.

#### SCALE COMPOSITION AND MICROSTRUCTURE

**Scale composition.**—Using Raman and fluorescence spectroscopy of chert-hosted fossils and energy-dispersive X-ray spectroscopy of macerated individuals, Cohen et al. (2011) documented the phosphatic nature of Fifteenmile scales and interpreted this as evidence of calcium phosphate biomineralization. High resolution SEM provides a detailed view of the microstructure and microfabric of the scale fossils. This is most clearly seen in specimens of *Characodictyon skolopium* (Fig. 19). The basal surface of *C. skolopium*, along with those other taxa that display hexagonally close-packed pores, consists of interwoven struts, each made up of bundled apatite fibers (Fig. 19.3, 19.4). There is some variation in size among fibers, but most are 300–900 nm long and 30–50 nm in cross-sectional diameter. The fibers are stiff and show no sign of deformation; broken tips of spines on *C. skolopium* (Fig. 19.1, 19.2) show that fiber terminations have been sheared clean. A different fractured specimen of *C. skolopium* shows that at least in some instances, the interwoven struts form flattened sheets, which may have facilitated the interfingering of struts (Fig. 19.6, 19.7, 19.8). In some specimens, individual apatite fibers are either not present or not visible (e.g., Fig. 15.2) whereas in others they are quite distinct (e.g., Fig. 19.4).

**Original composition.**—In the present day, scale biomineralization occurs by the deposition of silica, calcite or dahllite on and within a carbonaceous matrix (Weiner and Dove, 2003). Consistent with this, Fifteenmile scales show chemical evidence

of preserved organic carbon, as well as apatite. Several arguments have been advanced in favor of a primary phosphatic composition (Cohen et al., 2011). All scales, whether preserved in chert or limestone, have a similar composition; no purely organic and no silica-mineralized scales were observed. In contrast, no other microfossils in the Fifteenmile assemblage are preserved by phosphate; apatite mineralization is uniquely associated with the scale fossils (Cohen et al., 2011). Phosphatic scales display a finely resolved microstructure consistent with a primary depositional fabric and show no evidence for secondary phosphatic coatings. In addition, scales show little evidence of plastic deformation, an argument whose strength depends on the untested expectation that small organic scales would fold or bend upon burial.

Arguments in favor of penecontemporaneous phosphatization must account for these observations but studies of Cambrian embryos and small shelly fossils suggest that diagenetic phosphatization is potentially consistent with observed features. Phosphatization of embryos and small shelly fossils results in an apatite-organic carbon composition, can preserve fine-scale textures (Runnegar, 1985; Yao et al., 2011), and can be taxon specific (e.g., Creveling et al., 2011).

An additional argument in favor of diagenetic phosphatization is the extreme rarity of phosphate biomineralization in living protists (Knoll, 2003). Hedley et al. (1977) proposed that tests of the freshwater rhizarian *Cryptodiffugia oviformis* are lined with amorphous calcium phosphate (no scales), while Domozych et al. (1991) reported phosphatic scales in the freshwater green alga flagellate *Mesostigma viride*. The latter report is based on elemental analysis, making it difficult to rule out polyphosphate bodies as an alternate source of observed C and P enrichment (Raven and Knoll, 2010). If the observed phosphate is diagenetic,

the original scales must have been organic, as known calcite scales (largely coccoliths) do not have the fine morphological structure preserved in the fossils, there is no evidence of calcite pseudomorphs, and we know of no evidence for phosphate replacement of silica during diagenesis.

At present, both biomineralization and penecontemporaneous diagenetic mineralization provide plausible explanations for the Fifteenmile scales. Whether the Fifteenmile scales were mineralized in life or afterward, their current restriction to a single locality bears consideration. Possibly, phosphatic scales had a high probability of dissolution in pore fluids or local diagenetic mineralization may have preserved organic scales unlikely to escape decay in most sediments. It is also possible that because of a research focus on chert and shale, paleontologists have overlooked scale fossils in contemporaneous limestones and dolostones—a possibility easily testable by acid dissolution of other Neoproterozoic carbonates.

#### COMPARATIVE PALEOBIOLOGY

*Size reconstruction.*—The average diameter of the Fifteenmile scale fossils is 26.6  $\mu\text{m}$  with a maximum of 68.1  $\mu\text{m}$ , a minimum of 6.9  $\mu\text{m}$ , and a standard deviation of 11.3 (N=115). Preserved scale clusters provide something of a minimum estimate for the original total diameter of the organism, and these range from 30 to 80  $\mu\text{m}$  (Fig. 17; Allison and Hilgert, 1986). While the Fifteenmile scales bear some resemblance to organic and siliceous scales made by living organisms, no modern protist commonly makes scales as large as even the average diameter of the fossil taxa described here.

However, we can attempt to reconstruct whole organism size based on observed relationships between scale size and cell diameter in living protists (Fig. 20). Hendriks and colleagues (Henderiks and Pagani, 2007, 2008; Henderiks, 2008) provide equations for cell size and for total sphere diameter (cell plus scales) for coccolithophorids, based on measurement of a number of species. Significant differences in reconstructed size can occur due to the fact that some coccolithophores have relatively few, large plates, while others have many smaller plates. Thus, the estimates presented here should be viewed as broad constraints, potentially facilitating biological interpretation of the cells that fashioned Fifteenmile scales.

Our size estimates rest upon the assumption that the relationships between scales, cell diameter, and total sphere diameter (cell plus scales) can be extrapolated across potentially disparate taxa. With this in mind, we estimated total sphere diameter ranges from 30–210  $\mu\text{m}$  and total cell diameters (whole organism, minus scales) of 25–55  $\mu\text{m}$  for the taxa *Characodictyon skolopium*, *Thorakidictyon myriocanthum* n. comb., and *Paleohexadictyon litosum* emend. (Fig. 20). Because the larger estimates shown in Figure 20 are based on a coccolith group (the Syracosphaerales) with many small scales, it seems unlikely that the higher end of this model is correct; thus a more appropriate range for total sphere diameter is 30–140  $\mu\text{m}$ , though this cutoff is somewhat arbitrary.

While coccolith plates may have been larger in the past (Henderiks and Pagani, 2007; Henderiks and Pagani, 2008), even at their maximum they rarely grew larger than 14  $\mu\text{m}$ , significantly below the size of Fifteenmile scale fossils. Full coccosphere diameters are rarely greater than 16  $\mu\text{m}$  (Knappertsbusch, 2000; Henderiks and Pagani, 2007; Henderiks, 2008). The same pattern can be found in other modern analogs—the scales of prasinophyte green algae rarely grow larger than 2 to 3  $\mu\text{m}$  and the total diameter of the organism is usually under 10  $\mu\text{m}$  (Becker et al., 1994; Leroi and Hallegraeff, 2006). While many chrysophyte scales, synurophyte scales, and ciliate lepidosomes

have morphologies that broadly resemble Fifteenmile fossils, they also rarely exceed a few microns in maximum dimension (Douglas and Smol, 1987; Preisig, 1994; Foissner, 2005; Leroi and Hallegraeff, 2006), though total sphere diameter may be much larger, especially in ciliates. The centroheliid heliozoan *Raphidiophrys ambigua* may provide the best available modern analog with respect to size as its scales can reach lengths of up to 13  $\mu\text{m}$  and the maximum diameter of a single organism can exceed 60  $\mu\text{m}$  (Nicholls and Durrschmidt, 2008). However, most individual raphidiophyr scales are under 5  $\mu\text{m}$  in maximum dimension (Patterson and Durrschmidt, 1988; Nicholls and Durrschmidt, 2008). The large size of the Fifteenmile scales thus presents a challenge when attempting to reconstruct both their function and taxonomic affinity.

*Functional morphology.*—Functional interpretations of protist scales show little consensus, likely because scales play various roles in cell biology and ecology. A variety of functional explanations have been offered for the biomineralized scales of coccolithophores and other phytoplankton (Sikes and Wilbur, 1982; Young, 1994; Young et al., 1999). One common hypothesis is that the hard outer coverings protect cells from grazing. While this may be true for some biomineralizing plankton such as diatoms (Hamm et al., 2003), experimental work with coccolithophores and various metazoan zooplankton grazers shows that the grazers make little distinction between naked and covered cells (Sikes and Wilbur, 1982; Young, 1994). While this challenges the argument for defense against metazoan grazing, the same cell coverings may be highly effective in deterring protistan predators, which are widely distributed in marine and fresh waters. Predatory protists were abundant and diverse constituents of mid-Neoproterozoic marine communities (Porter et al., 2003; Porter, 2011). Molecular clocks also suggest that animals may have begun to diverge at this time (Erwin et al., 2011) but the size and functional capabilities of these Ur-metazoans would have been little different from those of their close protistan relatives (Dayel et al., 2011).

Protection against protistan predators may well have been a principal function of Fifteenmile scales. It is also possible that such coverings protected the enclosed cell from phage attack by restricting access to the protoplasm, one hypothesized function for diatom frustules (Raven and Waite, 2004; Losic et al., 2006). Additionally, cell coverings can provide mechanical protection against environmental effects, such as salinity change (Young, 1994).

Another likely function of biomineralized structures in protists is to alter the rate at which cells fall through the water column (Sikes and Wilbur, 1982; Young, 1994; Raven and Waite, 2004). Depending on the size of the cell and the number and density of the plates surrounding the cell, biomineralized plates can greatly increase the sinking rate of a cell. This is relevant to cell function because a cell that is stationary within the water column may quickly deplete the nutrients in its immediate surroundings. The increased sinking velocity caused by biomineralized cell coverings can be counterbalanced by turbulent mixing, reproduction, or buoyant vacuoles such as those found in the coccolithophore *E. huxleyi* (Young, 1994). These balancing effects can make relatively dense cell coverings a viable way to access heterogeneous resources within the water column without sinking to the seafloor.

Modern scale-bearing taxa generally form plates that either abut each other to cover the cell, or overlap. Abutting forms commonly have shapes that maximize close-packing, such as in the five-sided liths of the coccolithophore *Braarudosphaera bigelowii* (Bartol et al., 2008). A comparable arrangement seems likely for the Fifteenmile taxa *Hexacatillus allmonii* n. sp. and *Hexacatillus retetantillus* n. sp., whose hexagonal geometry

would have facilitated close-packing. Round and oval scales are better suited to an overlapping covering and, indeed, this can be observed in scales still preserved in clusters (Fig. 17). Square scales would probably overlap on a spherical cell but as demonstrated by the modern testate amoeba *Quadrullella quadrigera*, they can tile vase-shaped tests effectively. To the extent that scales protect against protistan predators, overlapping scales are advantageous because they guarantee complete coverage of the enclosed cell. However, this is achieved at the expense of greater resource use compared with abutting cells.

Further functional considerations focus on the hexagonal openings and ornament of preserved scales. The latticed surface structure of many Fifteenmile taxa may function like pores in diatom frustules, which allow the passage of gasses and nutrients between cell and environment and provide conduits for mucilage secretion (Kooistra et al., 2007), while decreasing the cost of construction; honeycomb-like surface patterns are widespread among the scales of extant protists (e.g., Domozych et al., 1991; Yoshida et al., 2006).

Spines also find counterparts among the scales made by modern protists. Some groups of coccolithophores such as *Rhabdosphaera* have a large spine emerging from the center of each plate (Hernández-Becerril et al., 2001), analogous to those seen in *Characodictyon skolopium* and *Quadrireticulum palmaspinosum* n. sp. (Figs. 6, 14). Scales made by siliceous haptophytes, ciliates, and green algae may also have boss-like central spines, increasing apparent cell diameter without greatly affecting cell density and, thus, slowing sinking (Sarjeant et al., 1987; Buckland-Nicks, 1993). Such a function is possible for Fifteenmile scales with large spines; of course, such structures may have also been effective against protistan predators. Studies of modern protist predators show that the ideal predator:prey size ratio varies from 1:1 in dinoflagellates to 10:1 in ciliates (Hansen et al., 1994). If the Fifteenmile taxa were prey to heterotrophic protists, larger apparent size would potentially lower predation rates.

**Mineralogical composition.**—Once an organism has evolved a cell covering, biomineralized coverings may be more advantageous than organic coverings because they can have a lower constructional cost (Raven, 1983; Young 1994). The cost of biomineralization is thought to relate to saturation state in the ambient environment for the mineral under consideration (Knoll, 2003). The phylogenetic distribution of biomineralizing clades shows that the ability to biomineralize has evolved many times through eukaryotic history (Knoll, 2003). In contrast, phosphatic biomineralization by protists is rare in general and unknown in the marine realm. Calcium phosphate minerals have low solubility in seawater, so low that animals require a battery of molecules to inhibit phosphate crystallization (e.g., Meyer et al., 1974), but carry a potential cost to photosynthetic cells in that they sequester a major nutrient. Photoautotrophs gain phosphate from seawater but the removal of this major nutrient to a relatively inaccessible reservoir may explain why algae don't mineralize using phosphate. Heterotrophs may gain phosphate from their diet; given Redfield ratios in their food, heterotrophic protists might then need an efficient pathway for nitrogen excretion to balance any phosphate sequestration.

It is possible, however, that clades utilized, and subsequently discarded, biomineralization pathways advantageous only during a past interval of Earth history. Regardless of the current rarity of phosphate mineralization in protistan scales, dahllite biomineralization could have been more prominent if  $[\text{PO}_4^{3-}]$  were more abundant in seawater and, at least for photosynthetic protists, not limiting for primary production. Planavsky et al. (2010) have argued for high phosphate in Neoproterozoic seawater, perhaps facilitated by anoxia in and above the seafloor (Ingall and Jahnki,

1994; Van Cappellen and Ingall, 1994). The high phosphate concentrations inferred from these analyses may record the composition of subsurface water masses, and if surface waters also had high phosphate levels, P was probably not limiting for primary production. Thus, it is possible that high phosphate availability permitted phosphate biomineralization of a type not observed in modern oceans. Phosphate biomineralization may have provided a temporally-bounded, low cost path for the formation of cell coverings by some Neoproterozoic protists. At present, the question must remain open.

#### PHYLOGENETIC PLACEMENT

External cell-covering scales are made by diverse living protists, including ciliates (Foissner, 2005), haptophytes (Yoshida et al., 2006), euglyphid rhizarians (Lara et al., 2007), testate lobose amoeba (Ogden and Hedley, 1980), chrysophytes and synurophytes (Preisig, 1994; Wujek and Bicudo, 2004), and green algae (Moestrup and Walne, 1979; Domozych et al., 1991). As no known modern organisms produce cell coverings of the same size and morphology as the Fifteenmile microfossils, and as convergence is rampant among modern scale-forming taxa, definitive taxonomic assignment is impossible. Based solely on size and morphology, the most promising alliance for many of the Fifteenmile microfossils is with the centrohelid heliozoa, a diverse protistan clade that includes the scale-forming raphidophyrs (Nicholls and Durrschmidt, 2008), or with the haptophytes (the clade that includes the calcareous coccolithophorids), their closest sister group (Keeling et al., 2005; Cavalier-Smith and von der Heyden, 2007). Modern arcellid testate amoeba also present a potential affinity—the testate amoeban *Quadrullella quadrigera* constructs vase-shaped tests about 100  $\mu\text{m}$  long that are armored by  $\sim 10 \mu\text{m}$  solid scales that are nearly perfect squares (Deflandre, 1936; see <http://tolweb.org/Quadrullella/124526>) similar to those seen in some Fifteenmile taxa. The scales of *Quadrullella* are siliceous, differentiating them from scales in the Fifteenmile assemblage, but they serve to remind us that testate amoebans, which can also form round and oval scales and whose mid-Neoproterozoic radiation is independently documented by vase-shaped microfossils (Porter and Knoll, 2000; Porter et al., 2003), provide candidate counterparts for many of the Fifteenmile assemblage. Based on composition, only the green alga *Mesostigma viride* has been reported to mineralize scales with Ca-phosphate, although as noted above this analysis warrants confirmation and the scales of this alga do not closely resemble Fifteenmile scales. Of course, if the apatite in the fossils is diagenetic in origin, current mineralogy places few constraints on phylogenetic affinity.

It is possible that the Fifteenmile microfossils record a now extinct group, potentially a stem clade, within or closely allied to the centrohelid heliozoa + Haptophyta (e.g., the Hacrobia, Okamoto et al., 2009). The phylogenetic placement of this group remains fluid but phylogenetic hypotheses tend to place them near the base of the great clade that includes Rhizaria, Alveolates and Stramenopiles (e.g., Yoon et al., 2004; Parfrey et al., 2010) or as sister to the green algae (e.g., Hampl et al., 2009). If we accept biomarker evidence for dinoflagellates (Summons and Walter, 1990) and both biomarker (Summons and Walter, 1990) and microfossil (Butterfield et al., 1994) evidence for green algae in ca. 800 Ma rocks, then we would conclude that Hacrobia clade had diverged by the time of Fifteenmile deposition. Recent molecular clock estimates support such a conclusion (e.g., Yoon et al., 2004; Berney and Pawlowski, 2006; Parfrey et al., 2011).



## CONCLUSIONS

The phosphatic scales of the Fifteenmile Group record 38 taxa of protists, making them the most diverse class of pre-Ediacaran eukaryotes. Along with the work of Bosak and colleagues (Bosak et al., 2011a, 2011b), these findings emphasize the importance of viewing the Neoproterozoic fossil record through as many preservational windows as possible to ensure full coverage of clades subject to diverse taphonomic biases. In addition, these findings also open up the possibility for additional fossil diversity in Neoproterozoic carbonates which have previously yielded abundant casts and molds of vase-shaped microfossils (e.g., Porter et al., 2003).

While the taxonomic affinities of the Fifteenmile Group fossils remain uncertain, the innovation of scaly cell coverings itself implies a changing ecological landscape in Neoproterozoic oceans. Predation has long been viewed as a principal driver of early animal diversification and has also been implicated in the radiation of plankton in the Cambrian (Vermeij, 1989; Butterfield, 1997). Predation by heterotrophic protists able to capture and ingest eukaryotic cells (see references in Cohen et al., 2009) may have played a similar role in facilitating eukaryotic diversification in early to mid-Neoproterozoic oceans. Vase-shaped protists provide direct evidence of protistan predators at this time (Porter et al., 2003; Porter, 2011) and the hypothesis is supported both by evidence of resistant cell-coverings in these microfossils and by a general diversification of eukaryotes and early metazoans at this time as inferred from fossils and molecular clocks (Berney and Pawłowski, 2006; Knoll et al., 2006; Macdonald et al., 2010a; Parfrey et al., 2011; Erwin et al., 2011). Thus, the advent of armored protist groups in pre-Sturtian seas may represent an evolutionary response to escalating ecological pressures and more complex ecosystem dynamics spurred by the radiation of major eukaryotic clades.

## ACKNOWLEDGMENTS

The authors thank S. Porter and S. Xiao for constructive and helpful reviews. PAC thanks L. Dalton for assistance in the lab. SEM studies were performed at the Harvard University Center for Nanoscale Systems (CNS), a member of the National Nanotechnology Infrastructure Network (NNIN), which is supported by NSF award no. ECS-0335765. PAC was funded by NSF grant EAR 0420592, the Cushman Foundation, a NSF GRFP award, and the NASA Astrobiology Institute.

## REFERENCES

- ALLISON, C. W. AND M. A. MOORMAN. 1973. Microbiota from the late Proterozoic Tindir Group, Alaska. *Geology*, 1:65–68.
- ALLISON, C. W. AND J. W. HILGERT. 1986. Scale microfossils from the early Cambrian of Northwest Canada. *Journal of Paleontology*, 60:973–1015.
- ALLISON, C. W. AND S. M. AWRAMIK. 1989. Organic-walled microfossils from earliest Cambrian or latest Proterozoic Tindir Group rocks, Northwest Canada. *Precambrian Research*, 43:253–294.
- BARTOL, M., J. PAVŠIČ, M. DOBNIKAR, AND S. M. BERNASCONI. 2008. Unusual Braarudosphaera bigelowii and Micrantholithus vesper enrichment in the Early Miocene sediments from the Slovenian Corridor, a seaway linking the Central Paratethys and the Mediterranean. *Palaeogeography, Palaeoclimatology, Palaeoecology*, 267:77–88.
- BECKER, B., B. MARIN, AND M. MELKONIAN. 1994. Structure, composition, and biogenesis of prasinophyte cell coverings. *Protoplasma*, 181:233–244.
- BERNEY, C. AND J. PAWŁOWSKI. 2006. A molecular time-scale for eukaryote evolution recalibrated with the continuous microfossil record. *Proceedings of the Royal Society B: Biological Sciences*, 273:1867–1872.
- BOSAK, T., F. MACDONALD, D. LAHR, AND E. MATYS. 2011a. Putative Cryogenian ciliates from Mongolia. *Geology*, 39:1123–1126.
- BOSAK, T., D. J. G. LAHR, S. B. PRUSS, F. A. MACDONALD, A. J. GOODAY, L. DALTON, AND E. D. MATYS. 2011b. Possible early foraminiferans in post-Sturtian (716–635 Ma) cap carbonates. *Geology*, 40:67–70.
- BUCKLAND-NICKS, J. 1993. Hull cupules of chiton eggs: parachute structures and sperm focusing devices? *The Biological Bulletin*, 184:269–276.
- BUTTERFIELD, N. J. 1997. Plankton ecology and the Proterozoic–Phanerozoic transition. *Paleobiology*, 23:247–262.
- VAN CAPPELLEN, P. AND E. D. INGALL. 1994. Benthic phosphorus regeneration, net primary production, and ocean anoxia: a model of the coupled marine biogeochemical cycles of carbon and phosphorus. *Paleoceanography*, 9:677–692.
- CAVALIER-SMITH, T. AND S. VON DER HEYDEN. 2007. Molecular phylogeny, scale evolution and taxonomy of centrohelid heliozoa. *Molecular Phylogenetics and Evolution*, 44:1186–1203.
- COHEN, P. A., A. H. KNOLL, AND R. B. KODNER. 2009. Large spinose microfossils in Ediacaran rocks as resting stages of early animals. *Proceedings of the National Academy of Sciences*, 106:6519–6524.
- COHEN, P. A., J. W. SCHOPF, N. J. BUTTERFIELD, A. B. KUDRYAVTSEV, AND F. A. MACDONALD. 2011. Phosphate biomineralization in mid-Neoproterozoic protists. *Geology*, 39:539–542.
- CREVELING, J., D. T. JOHNSTON, AND A. H. KNOLL. 2011. Geochemical controls on phosphatization taphonomy in the Middle Cambrian. *Geological Society of America, Abstracts with Programs*, 43(5):53.
- CROSS, L. AND J. M. FORTUNO. 2002. Atlas of northwestern Mediterranean coccolithophores. *Scientia Marina*, 66:7–182.
- DAYE, M. J., R. A. ALEGADO, S. R. FAIRCLOUGH, T. C. LEVIN, S. A. NICHOLS, K. MCDONALD, AND N. KING. 2011. Cell differentiation and morphogenesis in the colony-forming choanoflagellate *Salpingoeca rosetta*. *Developmental Biology*, 357:73–82.
- DEFLANDRE, G. 1936. Etude monographique sur le genre *Nebela* Leidy (Rhizopoda-Testacea). *Annals of Protistology*, 5:201–286.
- DOMOZYCH, D., B. WELLS, AND P. SHAW. 1991. Basket scales of the green-alga, *Mesostigma viride*—chemistry and ultrastructure. *Journal of Cell Science*, 100:397–407.
- DOUGLAS, M. AND J. SMOL. 1987. Siliceous protozoan plates in lake sediments. *Hydrobiologia*, 154:13–23.
- ERWIN, D. H., M. LAFLAMME, S. M. TWEEDT, E. A. SPERLING, D. PISANI, AND K. J. PETERSON. 2011. The Cambrian conundrum: early divergence and later ecological success in the early history of animals. *Science*, 334:109–1097.
- FOISSNER, W. 2005. Two new “flagship” ciliates (Protozoa, Ciliophora) from Venezuela: *Sleighophrys pustulata* and *Luporinophrys micelae*. *European Journal of Protistology*, 41:99–117.
- HAMM, C. E., R. MERKEL, O. SPRINGER, P. JURKOJC, C. MAIER, K. PRECHTEL, AND V. SMETACEK. 2003. Architecture and material properties of diatom shells provide effective mechanical protection. *Nature*, 421:841–843.
- HAMPL, V., L. HUG, J. W. LEIGH, J. B. DACKS, B. F. LANG, A. G. B. SIMPSON, AND A. J. ROGER. 2009. Phylogenomic analyses support the monophyly of Excavata and resolve relationships among eukaryotic “supergroups.” *Proceedings of the National Academy of Sciences*, 106:3859–3864.
- HANSEN, B., P. K. BJORNSEN, AND P. J. HANSEN. 1994. The size ratio between planktonic predators and their prey. *Limnology and Oceanography*, 39:395–403.
- HEDLEY, R., C. OGDEN, AND N. MORDAN. 1977. Biology and Fine Structure of *Cryptodiffugia Oviformis* (Rhizopoda: Protozoa). *British Museum (Natural History)*, London, 30 p.
- HENDERIKS, J. 2008. Coccolithophore size rules—Reconstructing ancient cell geometry and cellular calcite quota from fossil coccoliths. *Marine Micropaleontology*, 67:143–154.
- HENDERIKS, J. AND M. PAGANI. 2007. Refining ancient carbon dioxide estimates: significance of coccolithophore cell size for alkenone-based pCO<sub>2</sub> records. *Paleoceanography*, 22:PA3202, 12 p.
- HENDERIKS, J. AND M. PAGANI. 2008. Coccolithophore cell size and the Paleogene decline in atmospheric CO<sub>2</sub>. *Earth and Planetary Science Letters*, 269:576–584.
- INGALL, E. AND R. JAHNKE. 1994. Evidence for enhanced phosphorus regeneration from marine sediments overlain by oxygen depleted waters. *Geochimica et Cosmochimica Acta*, 58:2571–2575.
- KAUFMAN, A. J., A. H. KNOLL, AND S. M. AWRAMIK. 1992. Biostratigraphic and chemostratigraphic correlation of Neoproterozoic sedimentary successions; upper Tindir Group, northwestern Canada, as a test case. *Geology*, 20:181–185.
- KEELING, P., G. BURGER, D. DURNFORD, B. LANG, R. LEE, R. PEARLMAN, A. ROGER, AND M. GRAY. 2005. The tree of eukaryotes. *Trends in Ecology and Evolution*, 20:670–676.
- KNAPPERTSBUSCH, M. 2000. Morphological evolution of the coccolithophorid *Calcidiscus leptoporus* from the early Miocene to Recent. *Journal of Paleontology*, 74:712–730.
- KNOLL, A. H. 2003. Biomineralization and evolutionary history. *Reviews in Mineralogy and Geochemistry*, 54:329–356.
- KNOLL, A., E. JAVAUX, D. HEWITT, AND P. COHEN. 2006. Eukaryotic organisms in Proterozoic oceans. *Philosophical Transactions of the Royal Society B: Biological Sciences*, 361:1023–1038.

- KOOISTRA, W. H. C. F., R. GERSONDE, L. K. MEDLIN, AND D. G. MANN. 2007. The origin and evolution of the diatoms: their adaptation to a planktonic existence, p. 207–249. *In* P. Falkowski and A. H. Knoll (eds.), *The Evolution of Primary Producers in the Sea*. Elsevier, Burlington.
- LARA, E., T. J. HEGER, E. A. D. MITCHELL, R. MEISTERFELD, AND F. EKELUND. 2007. SSU rRNA reveals a sequential increase in shell complexity among the euglyphid testate Amoebae (Rhizaria: Euglyphida). *Protist*, 158:229–237.
- LEROI, J. AND G. HALLEGRAEFF. 2006. Scale-bearing nanoflagellates from southern Tasmanian coastal waters, Australia. II. Species of Chrysophyceae (Chrysophyta), Prymnesiophyceae (Haptophyta, excluding Chrysochromulina) and Prasinophyceae (Chlorophyta). *Botanica Marina*, 49:216–235.
- LEWIS, L. A. AND R. M. MCCOURT. 2004. Green algae and the origin of land plants. *American Journal of Botany*, 91:1535–1556.
- LOSIC, D., G. ROSENGARTEN, J. G. MITCHELL, AND N. H. VOELKER. 2006. Pore architecture of diatom frustules: potential nanostructured membranes for molecular and particle separations. *Journal of Nanoscience and Nanotechnology*, 6:982–989.
- MACDONALD, F. A., E. F. SMITH, J. V. STRAUSS, G. M. COX, G. P. HALVERSON, AND C. F. ROOTS. 2011. Neoproterozoic and early Paleozoic correlations in the western Ogilvie Mountains, Yukon, p. 161–182. *In* K. E. MacFarlane, L. H. Weston, and L. R. Blackburn (eds.), *Yukon Exploration and Geology 2010*. Yukon Geological Survey, Whitehorse.
- MACDONALD, F. A., M. D. SCHMITZ, J. L. CROWLEY, C. F. ROOTS, D. S. JONES, A. C. MALOOF, J. V. STRAUSS, P. A. COHEN, D. T. JOHNSTON, AND D. P. SCHRAG. 2010a. Calibrating the Cryogenian. *Science*, 327:1241–1243.
- MACDONALD, F. A., P. A. COHEN, F. O. DUDAS, AND D. P. SCHRAG. 2010b. Early Neoproterozoic scale microfossils in the lower Tindir Group of Alaska and the Yukon Territory. *Geology*, 38:143–146.
- MEYER, J. L., J. T. MCCALL, AND L. H. SMITH. 1974. Inhibition of calcium phosphate crystallization by nucleoside phosphates. *Calcified Tissue International*, 15:287–293.
- MOESTRUP, O. AND P. L. WALNE. 1979. Studies on scale morphogenesis in the Golgi apparatus of *Pyramimonas tetrahychnus* (Prasinophyceae). *Journal of Cell Science*, 36:437–459.
- NICHOLLS, K. AND M. DURRSCHMIDT. 2008. Scale structure and taxonomy of some species of Raphidocystis, Raphidiophrys, and Pompholyxophrys (Heliozoa) including descriptions of six new taxa. *Canadian Journal of Zoology*, 18:1944–1961.
- OGDEN, C. AND R. HEDLEY. 1980. *An Atlas of Freshwater Testate Amoebae*. Oxford University Press, Oxford, 282 p.
- OKAMOTO, N., C. CHANTANGSI, A. HORÁK, B. S. LEANDER, AND P. J. KEELING. 2009. Molecular phylogeny and description of the novel katablepharid *Roombia truncata* gen. et sp. nov., and establishment of the Hacrobria taxon nov. *PLoS ONE*, 4(9):e7080.
- PARFREY, L. W., J. GRANT, Y. I. TEKLE, E. LASEK-NESSELQUIST, H. G. MORRISON, M. L. SOGIN, D. J. PATTERSON, AND L. A. KATZ. 2010. Broadly sampled multigene analyses yield a well-resolved eukaryotic tree of life. *Systematic Biology*, 59:518–533.
- PARFREY, L., D. LAHR, A. H. KNOLL, AND L. A. KATZ. 2011. Estimating the timing of early eukaryotic diversification with multigene molecular clocks. *Proceedings of the National Academy of Sciences*, 108:13624–13629.
- PATTERSON, D. AND M. DURRSCHMIDT. 1988. The formation of siliceous scales by *Raphidiophrys ambigua* (Protista, Centroheliozoa). *Journal of Cell Science*, 91:33–39.
- PLAVANSKY, N. J., O. J. ROUXEL, A. BEKKER, S. V. LALONDE, K. O. KONHAUSER, C. T. REINHARD, AND T. W. LYONS. 2010. The evolution of the marine phosphate reservoir. *Nature*, 467:1088–1090.
- PORTER, S. 2011. The rise of predators. *Geology*, 39:607–608.
- PORTER, S., R. MEISTERFELD, AND A. KNOLL. 2003. Vase-shaped microfossils from the Neoproterozoic Chuar Group, Grand Canyon: a classification guided by modern testate amoebae. *Journal of Paleontology*, 77:409–429.
- PREISIG, H. 1994. Siliceous structures and silicification in flagellated protists. *Protoplasma* 181:29–42.
- RAVEN, J. A. 1983. The transport and function of silicon in plants. *Biological Reviews*, 58:179–207.
- RAVEN, J. A. AND A. H. KNOLL. 2010. Non-Skeletal biomineralization by eukaryotes: matters of moment and gravity. *Geomicrobiology Journal*, 27:572–584.
- RAVEN, J. A. AND A. M. WAITE. 2004. The evolution of silicification in diatoms: Inescapable sinking and sinking as escape? *New Phytologist*, 162:45–61.
- RUNNEGAR, B. 1985. Shell microstructures of Cambrian molluscs replicated by phosphate. *Alcheringa: An Australasian Journal of Palaeontology*, 9:245–257.
- SARJEANT, W., T. LACALLI, AND G. GAINES. 1987. The cysts and skeletal elements of dinoflagellates: Speculations on the ecological causes for their morphology and development. *Micropaleontology*, 33:1–36.
- SIKES, C. S. AND K. M. WILBUR. 1982. Functions of Coccolith Formation. *Limnology and Oceanography*, 27:18–26.
- SUMMONS, R. E. AND M. R. WALTER. 1990. Molecular fossils and microfossils of prokaryotes and protists from Proterozoic sediments. *American Journal of Science*, 290A: 212–244.
- VERMEIJ, G. J. 1989. The origin of skeletons. *Palaaios*, 4:585–589.
- WEINER, S. AND P. M. DOVE. 2003. An overview of biomineralization processes and the problem of the vital effect. *Reviews in Mineralogy and Geochemistry*, 54:1–29.
- WUJEK, D. AND C. BICUDO. 2004. Scale-bearing chrysophytes from the State of São Paulo, Brazil, 2: additions to the flora. *Brazilian Journal of Biology*, 64:915–918.
- YAO, X., J. HAN, AND G. JIAO. 2011. Early Cambrian epibolic gastrulation: A perspective from the Kuanchuanpu Member, Dengying Formation, Ningqiang, Shaanxi, South China. *Gondwana Research*, 20:844–851.
- YOON, H. S., J. D. HACKETT, C. CINIGLIA, G. PINTO, AND D. BHATTACHARYA. 2004. A molecular timeline for the origin of photosynthetic eukaryotes. *Molecular and Biological Evolution*, 21:809–818.
- YOSHIDA, M., M. NOEL, T. NAKAYAMA, T. NAGANUMA, AND I. INOUE. 2006. A haptophyte bearing siliceous scales: ultrastructure and phylogenetic position of *Hyalolithus neolepis* gen. et sp. nov. (Prymnesiophyceae, Haptophyta). *Protist*, 157:213–234.
- YOUNG, J. R., S. A. DAVIS, P. R. BOWN, AND S. MANN. 1999. Coccolith ultrastructure and biomineralisation. *Journal of Structural Biology*, 126:195–215.
- YOUNG, J. 1994. Functions of coccoliths, p. 63–82. *In* *Coccolithophores*. Cambridge University Press, Cambridge, United Kingdom.

ACCEPTED 3 APRIL 2012